HAW HAMBURG

Project

Possibilities and Limitations Using Flightradar24, ADS-B and Mode S Data for Aircraft Performance Analysis – an Overview

Author: Tim Maximilian Jansen

Supervisor: Prof. Dr.-Ing. Dieter Scholz, MSME
Submitted: 2020-03-25

Faculty of Engineering and Computer Science
Department of Automotive and Aeronautical Engineering

DOI:
https://doi.org/10.15488/xxxxx

URN:
https://nbn-resolving.org/urn:nbn:de:gbv:18302-aero2020-03-25.02
Associated URLs:
https://nbn-resolving.org/html/urn:nbn:de:gbv:18302-aero2020-03-25.02

Any further request may be directed to:
Prof. Dr.-Ing. Dieter Scholz, MSME
E-Mail see: http://www.ProfScholz.de

This work is part of:
Digital Library - Projects & Theses - Prof. Dr. Scholz
http://library.ProfScholz.de

Published by
Aircraft Design and Systems Group (AERO)
Department of Automotive and Aeronautical Engineering
Hamburg University of Applied Science

This report is deposited and archived:
- Deutsche Nationalbiliothek (https://www.dnb.de)
- Repositorium der Leibniz Universität Hannover (https://www.repo.uni-hannover.de)
- Internet Archive (https://archive.org)
  Item: https://archive.org/details/TextJansen.pdf

This report has associated published data in Harvard Dataverse:
https://doi.org/10.7910/DVN/D2DCBF

Abstract

Automatic dependent surveillance-broadcast, short ADS-B, is used for surveillance purposes by air traffic control. Besides that, it is used by flight tracking services and also gains popularity among private users. In this project, different sources of aircraft and flight data are discussed. On the one hand, the data provided by the flight tracking service Flightradar24. Different cases, each representing another possible aircraft performance or flight analysis, are presented and it is evaluated whether Flightradar24 data is suitable for this analysis. To demonstrate the value of Flightradar24 data, a study of initial cruise altitude and step climbs with 440 data sets of different aircraft types is conducted and the first findings are derived. On the other hand, a homebuilt receiver for ADS-B and other Mode S data is used. The technology behind ADS-B is presented and a decoding script for ADS-B and Comm-B messages, based on the open-source python library *pyModeS*, is developed. The potential of this data source is shown by analyzing flight data from an aircraft using the homebuilt set-up. The different sources are compared, and the results show that the data sources differ significantly in terms of the number of parameters, data rate, and coverage. Finally, a recommendation of data sources for different fields of application is proposed.

Content

Page

List of Figures 6
List of Tables 7
List of Symbols 8
List of Abbreviations 9
List of Definitions 10

1 Introduction 11
1.1 Motivation 11
1.2 Definitions 11
1.3 Objectives 11
1.4 Literature 12
1.5 Structure 12

2 State of the Art 13
2.1 Automatic Dependent Surveillance-Broadcast (ADS-B) 13
2.2 Flightradar24 14

3 Evaluation of Cases 15
3.1 Flightradar24 Data 15
3.2 Aborted Take-Off 15
3.3 Altitude and Speed during Holdings 17
3.4 Taxi Time 19
3.5 Altitude and Speed during Cruise Flight 21
3.6 Initial Cruise Altitude and Step Climbs 22
3.7 Discussion of the Cases 23

4 Initial Cruise Altitude and Step Climb Analysis 24
4.1 Breguet Range Equation 24
4.2 Data Acquisition 25
4.2.1 Flight Data 25
4.2.2 Airport Data 25
4.3 Data Preparation 25
4.3.1 Distance between Origin and Destination Airport 26
4.3.2 Track between Origin and Destination Airport 26
4.3.3 Determination of Cruise Altitudes and Step Climbs 26
4.3.4 Detection and Handling of Flight Data Interruptions 27
4.4 Analysis and Results 28
4.4.1 Initial Cruise Altitude 29
4.4.2 Step Climbs 33

4.4.3 Wide-body Aircraft Type Statistics 37
4.4.4 Cruise Altitudes 40
4.5 Discussion of the Analysis 42

5 ADS-B and Extended Mode S Data 43
5.1 ADS-B Message Types 44
5.2 Comm-B Replies 46
5.3 Receiving Equipment 48
5.3.1 Receiver Hardware 48
5.3.2 Decoding Software 49
5.4 Example Data 49
5.5 Discussion of ADS-B and Mode S Data 58

6 Summary and Conclusion 60

References 62

List of Figures

Figure 2.1 Flightradar24 coverage map November 2019 (Flightradar24 2019a) 14
Figure 3.1 Ground speed and altitude during aborted take-off run 16
Figure 3.2 Ground speed and altitude during multiple holdings 17
Figure 3.3 Track during multiple holdings 18
Figure 3.4 Flightradar24 playback of the considered holding pattern (Flightradar24 2019b) 19
Figure 3.5 Aircraft position and additional data during taxiing 20
Figure 3.6 Altitude and ground speed progression during a flight from Edmonton (YEG/CYEG) to Toronto (YYZ/CYYZ) 21
Figure 3.7 Altitude progression of an example flight from Frankfurt to Bangkok 22
Figure 4.1 Initial cruise altitude relative to great circle distance of selected narrow-body aircraft types 30
Figure 4.2 Initial cruise altitude relative to great circle distance of selected Airbus wide-body aircraft types 31
Figure 4.3 Initial cruise altitude relative to great circle distance of selected Boeing wide-body aircraft types 32
Figure 4.4 Number of step climbs relative to great circle distance of selected narrow-body aircraft types 34
Figure 4.5 Number of step climbs relative to great circle distance of selected Airbus wide-body aircraft types 35
Figure 4.6 Number of step climbs relative to great circle distance of selected Boeing wide-body aircraft types 36
Figure 4.7 Number of step climbs per 1000 km 37
Figure 4.8 Altitude difference during step climb 38
Figure 4.9 Time between step climbs 39
Figure 4.10 Vertical speed during step climbs 40
Figure 4.11 Cruise altitudes related to the track between origin and destination airport 41
Figure 5.1 Aircraft flight path in relation to origin airport and receiver location 51
Figure 5.2 Altitude information 52
Figure 5.3 Barometric pressure setting 53
Figure 5.4 Vertical Rate 53
Figure 5.5 Speed information 54
Figure 5.6 Heading information 55
Figure 5.7 Roll angle 56
Figure 5.8 Airborne status 56
Figure 5.9 Autopilot status 57
Figure 5.10 VNAV mode status 57
Figure 5.11 Altitude hold mode status 57
Figure 5.12 Approach mode status 58

List of Tables

Table 3.1 Overview of Flightradar24's CSV file contents 15
Table 4.1 Overview of analyzed flights per aircraft type 28
Table 5.1 Downlink Format Overview (adapted from EASA CS-ACNS) 43
Table 5.2 ADS-B Message Types (DF 17) (adapted from EASA CS-ACNS) 44
Table 5.3 ADS-B messages and corresponding parameters (adapted from EASA CS-ACNS and ICAO 9871) 45
Table 5.4 Broadcast rates of ADS-B messages in airborne state (adapted from ICAO 9871) 46
Table 5.5 Comm-B messages and corresponding parameters or information (ELS) (adapted from EASA CS-ACNS) 46
Table 5.6 Comm-B messages and corresponding parameters (EHS) (adapted from EASA CS-ACNS and ICAO 9871) 46
Table 5.7 Comm-B messages and corresponding parameters (other registers) (adapted from EASA CS-ACNS and ICAO 9871) 47
Table 5.8 Breakdown of received ADS-B messages 50
Table 5.9 Breakdown of received Comm-B messages 50

List of Symbols

c	specific fuel consumption
c_L	lift coefficient
E	glide ratio
g	acceleration of free fall
h	altitude
m	aircraft mass
M	Mach number
p	pressure
R	still air range
ROC	rate of climb
S	wing surface
V	velocity

Greek Symbols

Δ	difference
ρ	air density
σ	standard deviation

Indices

ic	initial cruise
GC	great circle
L	landing
TO	take-off

List of Abbreviations

ADS-B	automatic dependent surveillance-broadcast
CSV	comma-separated values
FMS	flight management system
FCU	flight control unit
GNSS	global navigation satellite system
GS	ground speed
IAS	indicated airspeed
MCP	mode control panel
RVSM	reduced vertical separation minimum
SSR	secondary surveillance radar
TA	transition altitude
TAS	true airspeed
TCP	transmission control protocol
UAT	universal access transceiver
VNAV	vertical navigation

List of Definitions

ADS-B
“ADS-B refers to automatic dependent surveillance-broadcast, a surveillance technique in which aircraft automatically provide, via a data link, data derived from on-board navigation and position-fixing systems. It refers to a surveillance technology where ADS-B Out equipped aircraft broadcast position, altitude, velocity, and other information in support of both air-to-ground and air-to-air surveillance applications.” (EASA CS-ACNS)

Comm-B
“Comm-B refers to a 112-bit Mode S reply containing a 56-bit MB message field containing the extracted transponder register.” (EASA CS-ACNS)

Downlink
“Downlink is a transfer of information, generated by an aircraft (not necessarily airborne) and sent to the ground for further processing by an ATC Centre.” (EASA CS-ACNS)

Mode S Elementary Surveillance (ELS)
“Mode S Elementary Surveillance refers to the use of Mode S surveillance data to downlink aircraft information from airborne installations.” (EASA CS-ACNS)

Mode S Enhanced Surveillance (EHS)
“Mode S Enhanced Surveillance refers to the use of other airborne information in addition to data used for Elementary Surveillance.” (EASA CS-ACNS)

Transponder
“Transponder is a device that transmits airborne surveillance data spontaneously or when requested. The transmissions are performed on 1090 MHz RF band and the interrogations are received on 1030 MHz RF band using SSR/Mode S protocols. It is also named Secondary Surveillance Radar transponder.” (EASA CS-ACNS)

Transponder register
“Transponder register is a transponder data buffer containing different pieces of information. It has 56 bits which are split in different fields. … Transponder registers are numbered in hexadecimal (00hex to FFhex). The register number is also known as the BDS code (Comm-B data selector).” (EASA CS-ACNS)

Uplink
“Uplink is a transfer of information, issued from any ground-based entity (typically: the ATC Centre under which the aircraft is under responsibility) to an aircraft (not necessarily airborne).” (EASA CS-ACNS)

1 Introduction

1.1 Motivation

During the flight, aircraft generate a tremendous amount of data. Access to this data is limited as airframers and airlines are restrictive. Flight tracking services like Flightradar24 use publicly available ADS-B and Mode S data to provide information about flights to its users. In most cases, this data is provided by users via home-based receivers. This project aims at presenting and evaluating the different data sources for flight and aircraft data. Besides, a general overview of the technology behind the data, possibilities and limitations shall be pointed out. An indication for the range of application for the data sources shall give guidance and help to select the most suitable one for a specific purpose.

1.2 Definitions

Flightradar24
Flightradar24 refers to a flight tracking service providing aircraft and flight information, mainly based on ADS-B and Mode S data. Further explanation is given in Chapter 2.

ADS-B
Automatic dependent surveillance-broadcast (ADS-B) refers to a technology that uses onboard systems to derive information and periodically sends this data to the ground for surveillance purposes. Further explanation is given in Chapter 2.

Mode S
Mode S refers to a secondary surveillance radar (SSR) interrogation mode that enables selective communication with individual aircraft. Further explanation is given in Chapter 5.

1.3 Objectives

This project shall give an overview of potential cases that could be analyzed using flight data provided by Flightradar24. A more comprehensive study regarding initial cruise altitudes and step climbs shall be conducted to demonstrate the value and limitations of this data source. Further, an overview of ADS-B and Comm-B messages shall be given. A python script, based on an open-source ADS-B and Mode S library, shall be developed for the decoding of this data. The possibilities of these flight data shall then be demonstrated by analyzing an example flight.

Finally, a comparison of the data sources, presenting their possibilities and limitations, shall be given.

1.4 Literature

Sun 2019 developed an innovative method to determine the BDS registers contained in Comm-B replies. This enables the decoding of these messages and therefore permitting access to a more considerable number of parameters and data, in addition to ADS-B messages. The authors published the decoding means in an open-source python library. In Chapter 5 of this project, the library serves as the basis for the development of a decoding script.

1.5 Structure

Chapter 2 presents the state of the art of this topic.

Chapter 3 shall give an overview of potential flight and aircraft performance analysis cases and discuss whether Flightradar24 data can be used to analyze these.

Chapter 4 shows a more comprehensive analysis of the cases *initial cruise altitude and step climbs*. A larger number of flight data of various aircraft types is used to find correlations between aircraft type, flight distance, initial cruise altitude and step climbs.

Chapter 5 shall give a more general overview of ADS-B and Comm-B messages sent via Mode S transponders. Furthermore, the data of an example flight received and decoded via a homebuilt receiving set-up is prepared and analyzed.

Chapter 6 gives a summary and a conclusion.

2 State of the Art

2.1 Automatic Dependent Surveillance-Broadcast (ADS-B)

> *"Automatic Dependent Surveillance-Broadcast (ADS-B) is a system broadcasting, without the need for action from the pilot or any request from ATC, that provides an enhanced set of aircraft surveillance data to Air Traffic Management (and potentially to other airplanes)." (EASA 2018a)*

This ADS-B data is derived from onboard systems and can be received from ground stations for surveillance purposes (ADS-B Out) and from other aircraft to "facilitate airborne traffic situational awareness" (Skybrary 2020a) (ADS-B In).

This technology "is seen as is seen as a key enabler of the future ATM Network on both sides of the North Atlantic and elsewhere and will be vital to the achievement of the Single European Sky (SES) and Next Gen performance objectives, including safety, capacity, efficiency and environmental sustainability." (Skybrary 2020a) This is, among others, due to the wide coverage and cost-efficiency.

As of 7th June 2020, the EASA requires all aircraft operating under instrument flight rules (IFR) to be equipped with Mode S Elementary Surveillance (ELS). Aircraft with a maximum take-off mass of more than 5,700 kg or a maximum true airspeed in cruise flight of 250 kt need to be equipped with Mode S Enhanced Surveillance (EHS) and ADS-B technology. More details on Mode S ELS and EHS, as well as ADS-B, are presented in Chapter 5 of this project. In several other regions, ADS-B has already been implemented or corresponding mandates are in place. (Skybrary 2020a)

This implementation opens up more possibilities to obtain flight data and also creates new business cases for flight tracking services like Flightradar24. As seen in Chapter 5, this data can also be received publicly using a homebuilt receiver.

2.2 Flightradar24

Flightradar24 uses a network of more than 20,000 terrestrial ADS-B receivers worldwide to receive flight data from aircraft equipped with a capable transponder. To add coverage in regions where flight tracking via terrestrial receivers is not possible, Flightradar24 uses data from other providers coming from satellites equipped with ADS-B receivers. Besides, multilateration (MLAT) is used to calculate the position of aircraft not equipped with an ADS-B transponder. In North America, Flightradar24 also uses live radar data. (Flightradar24 2020a)

With more aircraft equipped with ADS-B transponders and a growing network of ADS-B receivers, the number of flights being tracked by Flightradar24 increases. Flightradar24 stated that it has tracked a total of 68,948,849 flights in 2019, averaging to nearly 189,000 flights per day. (Flightradar24 2020b) Figure 2.1 shows the coverage of Flightradar24 in November 2019.

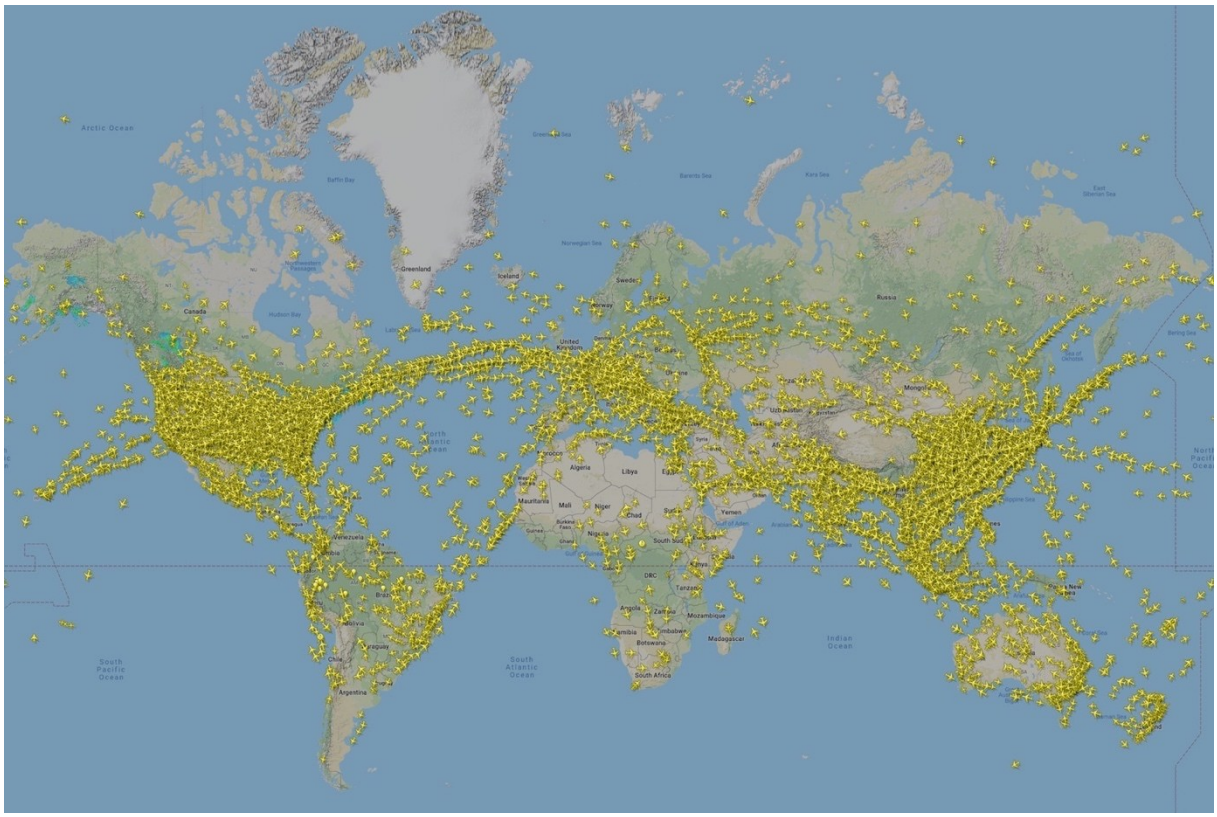

Figure 2.1 Flightradar24 coverage map November 2019 (Flightradar24 2019a)

3 Evaluation of Cases

3.1 Flightradar24 Data

Flightradar24 offers a complimentary Business subscription to those feeding data via their home-based ADS-B receiver. This entitles members to download up to 60 comma-separated values (CSV) files containing flight data of a specific flight of the last 720 days per day (Flightradar24 2020c). Table 3.1 gives an overview of the data contained in the CSV files.

Table 3.1 Overview of Flightradar24's CSV file contents

Column name	Content	Remark
Timestamp	Unix time	-
UTC	UTC date and time	-
Callsign	Callsign	-
Position	Latitude and longitude	-
Altitude	Pressure altitude	relative to standard pressure of 1013.25 hPa and with a resolution of 25 ft
Speed	Ground speed in kt	-
Direction	Track in °	calculated from east-west and north-south ground speed components

For the examination of the following cases only this data has been used. The data for every case is stored in the spreadsheet *FR24_Cases.xlsx* and is published on Harvard Dataverse. The download link can be found on page 2 of this project.

3.2 Aborted Take-Off

Looking at aborted take-offs it could be of interest to take a closer look at the aircraft speed during the take-off run. The speed at which the aircraft starts to decelerate, the maximum speed during the take-off run, could determine whether the decision speed V1 has been exceeded (provided that V1 information is available).

The only parameter needed for this determination, except for the corresponding timestamp, is the ground speed.
Figure 3.1 shows the progression of ground speed and altitude during an aborted take-off due to a bird strike of an Airbus A320 at London Southend airport. (Avherald 2019)

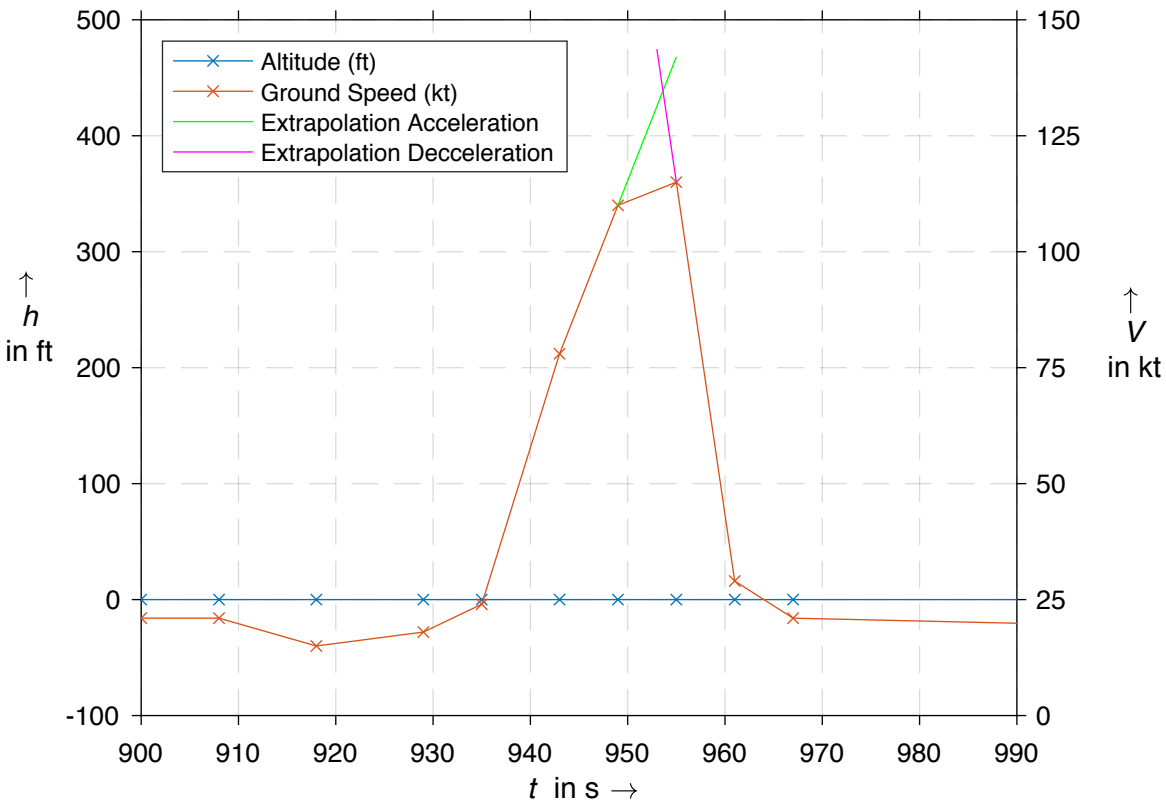

Figure 3.1 Ground speed and altitude during aborted take-off run

t	Time since first contact
h	Altitude
V	Velocity

It can be seen that the aircraft stays on the ground as the altitude remains 0 ft. At about 935 seconds after the first contact, the take-off run is initiated. The aircraft accelerates and reaches a ground speed of approx. 110 kt at 949 s. The next available data point shows a ground speed of 115 kt at 955 s. Thereafter, the aircraft decelerates to taxi speed. Therefore, it can be assumed that the maximum speed is reached between the two available data points at 949 s and 955 s.

Using a linear extrapolation for the acceleration and deceleration phase, it is possible to estimate a range for the maximum speed during the take-off run. In this example, the estimation leads to a maximum ground speed of up to approx. 130 kt.

3.3 Altitude and Speed during Holdings

This case shall take a closer look at the altitude and speed during holding patterns. Figure 3.2 shows the progression of the altitude and the ground speed during several holding patterns at London Heathrow Airport (LHR/EGLL). The holdings are discernible in Figure 3.3 as the track of the aircraft changes. Also, it can be observed that the ground speed changes with the track because of the changing wind velocity component.

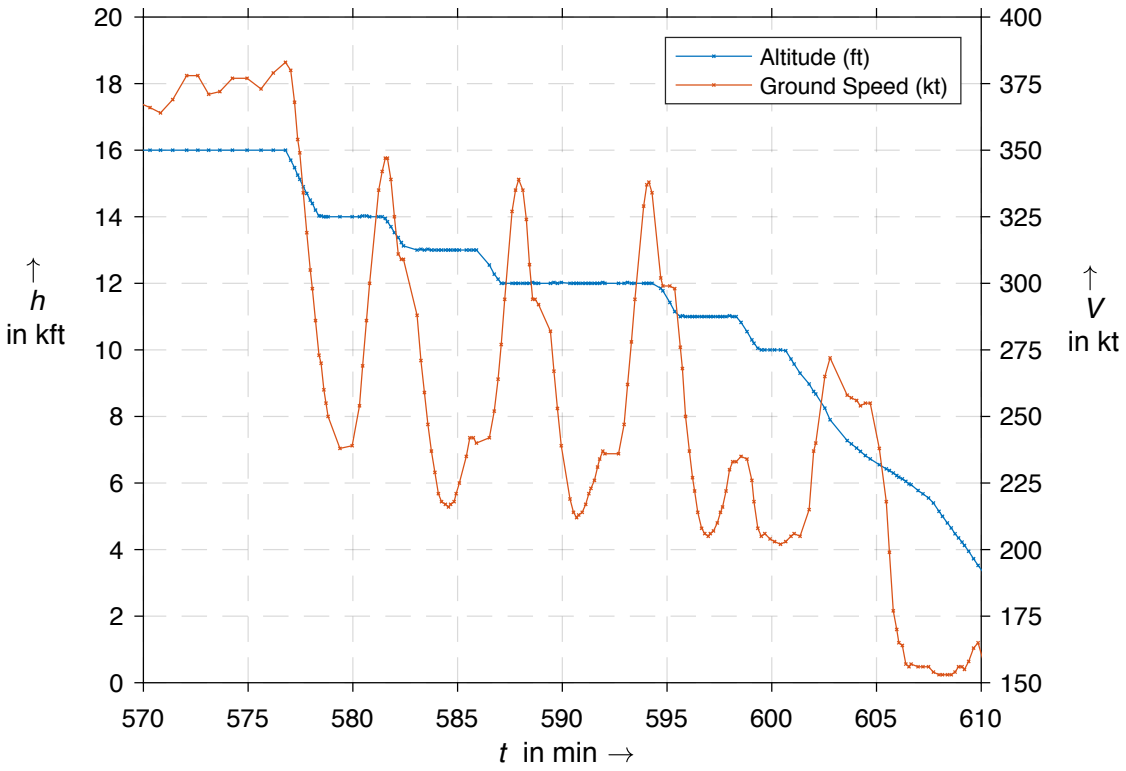

Figure 3.2 Ground speed and altitude during multiple holdings

t Time since first contact
h Altitude

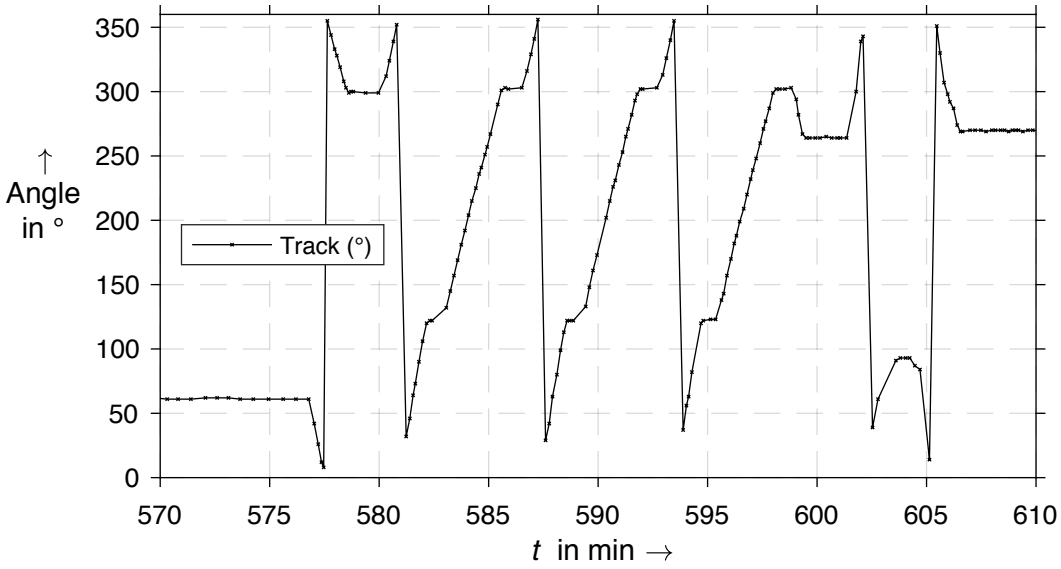

Figure 3.3 Track during multiple holdings

t Time since first contact

Within the considered time frame, the aircraft performs a total of three full holding patterns, i.e. the aircraft makes a 360° turn. The first holding pattern begins at approx. 580 min after the first contact at a track of 300° and an altitude of 14,000 ft. During the three holding patterns, the aircraft descends to an altitude of 11,000 ft. Each of the holding patterns has a duration of about six minutes.

As the aircraft performs a 360° turn, ground speed information is available for several track angles between 0° and 359° depending on the number of data points available. This gives the possibility to estimate the velocity and the direction of the wind as well as the true airspeed (TAS). As can be seen in Figure 3.2 and Figure 3.3, the aircraft reaches a maximum ground speed of approx. 347 kt at a track angle of 64°. At this time the wind should come from the opposite direction compared to the aircraft's track. The aircraft reaches its minimum ground speed of 216 kt at a track angle of 236° during the first holding pattern. During the two following holding patterns, similar behavior can be observed. The estimation leads to a wind velocity of about 66 kt from west-southwestern direction (approx. between 236° and 244°) and a true airspeed of approx. 282 kt.

Figure 3.4 shows the Flightradar24 playback of the flight. Here, the true airspeed of 282 kt is also indicated. This shows that a good estimation of the true airspeed considering the ground speed at different track angles during a holding pattern is possible.

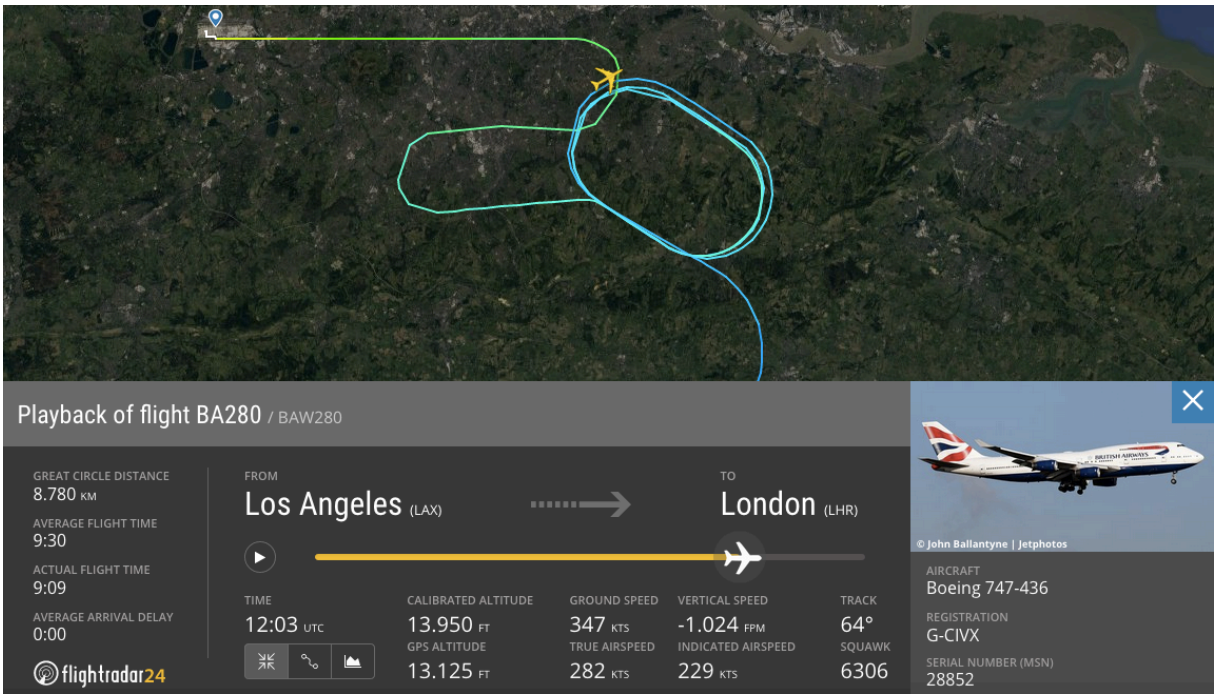

Figure 3.4 Flightradar24 playback of the considered holding pattern (Flightradar24 2019b)

3.4 Taxi Time

In this case, the taxi time of an aircraft shall be examined. For this analysis, the timestamp, as well as the position of the aircraft, is needed. As an example, a flight departing from London Heathrow Airport (LHR/EGLL) is considered. Figure 3.5 shows the taxi path from Terminal 5 to runway 09R. The altitude, ground speed, and timestamp are indicated for selected positions.

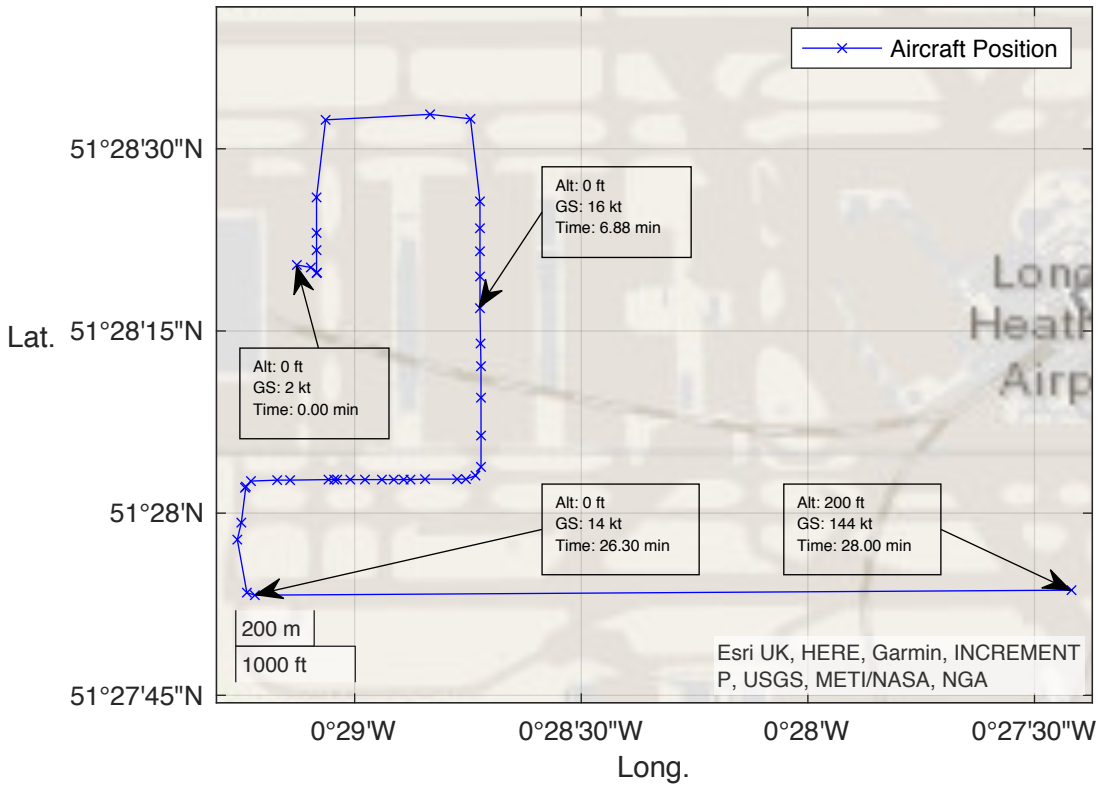

Figure 3.5 Aircraft position and additional data during taxiing

Long. Longitude
Lat. Latitude

It can be seen that enough data points are available to follow the taxiing of the aircraft. Between 6.88 min and 26.30 min, the number of available data points is greater than between the first contact of the aircraft at 0 min and 6.88 min. Also considering the significantly larger period for approx. the same taxi distance, it can be assumed that the aircraft had to queue on the taxiway due to traffic.

During the considered time frame, the data show that the aircraft reached a maximum speed of 34 kt and around 16 kt on average. Furthermore, it can be seen that no data is available during the take-off run. The next available data point is at an altitude of 200 ft, 28 minutes after the aircraft left its parking position at Terminal 5. At this time, the aircraft is already airborne. Therefore, the total taxi time at the origin airport amounts to 26.30 minutes.

It should be mentioned that surface position messages do not contain altitude information. Therefore, the data show an altitude of 0 ft while the aircraft is on the ground despite an airport elevation of 83 ft (**Skybrary 2020b**). Further details regarding the ADS-B message types and their contents are discussed in Chapter 5.1.

3.5 Altitude and Speed during Cruise Flight

This case shall illustrate and evaluate the possibility to use Flightradar24 data to gain information about altitude and speed during cruise flight phase. As an example, Figure 3.6 shows the altitude and ground speed of a flight from Edmonton (YEG/CYEG) to Toronto (YYZ/CYYZ).

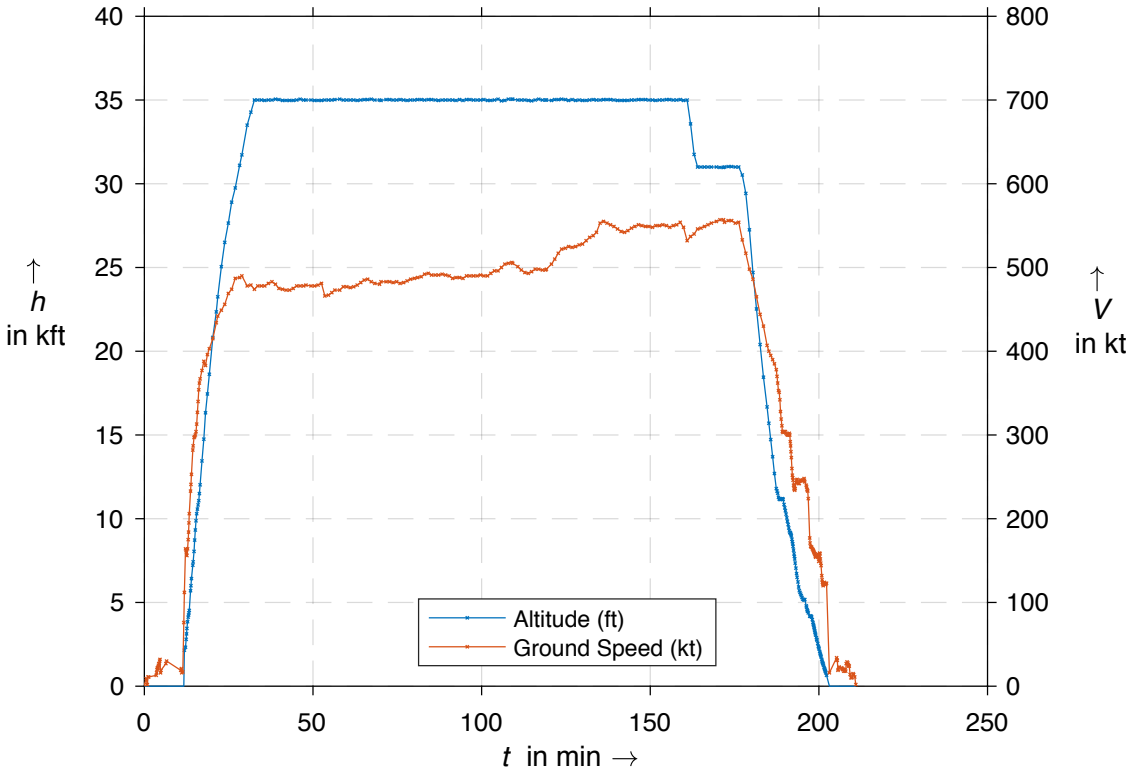

Figure 3.6 Altitude and ground speed progression during a flight from Edmonton (YEG/CYEG) to Toronto (YYZ/CYYZ)

t	Time after first contact
h	Altitude
V	Velocity

It can be noted that the cruise phase lasts from approx. 35 min when the aircraft reaches its cruise altitude of 35,000 ft and 175 min when the continuous descend towards the destination airport is initiated. For the last 12 minutes of the cruise flight phase, the aircraft remains at an altitude of 31,000 ft.

Taking a look at the ground speed during this phase, it can be seen that it ranges between 466 kt and 557 kt. Unlike the altitude, the ground speed shows a significant variation throughout the cruise flight phase. As the ground speed is the vector sum of the true airspeed and the wind velocity and no wind information is provided, no statement about the true airspeed is possible.

3.6 Initial Cruise Altitude and Step Climbs

For the determination of the initial cruise altitude as well as the step climbs only the altitude and the corresponding timestamp are needed. Figure 3.7 shows the progression of the altitude of an example flight from Frankfurt to Bangkok in December 2019. In this example, there are enough data points to determine the different altitude steps.

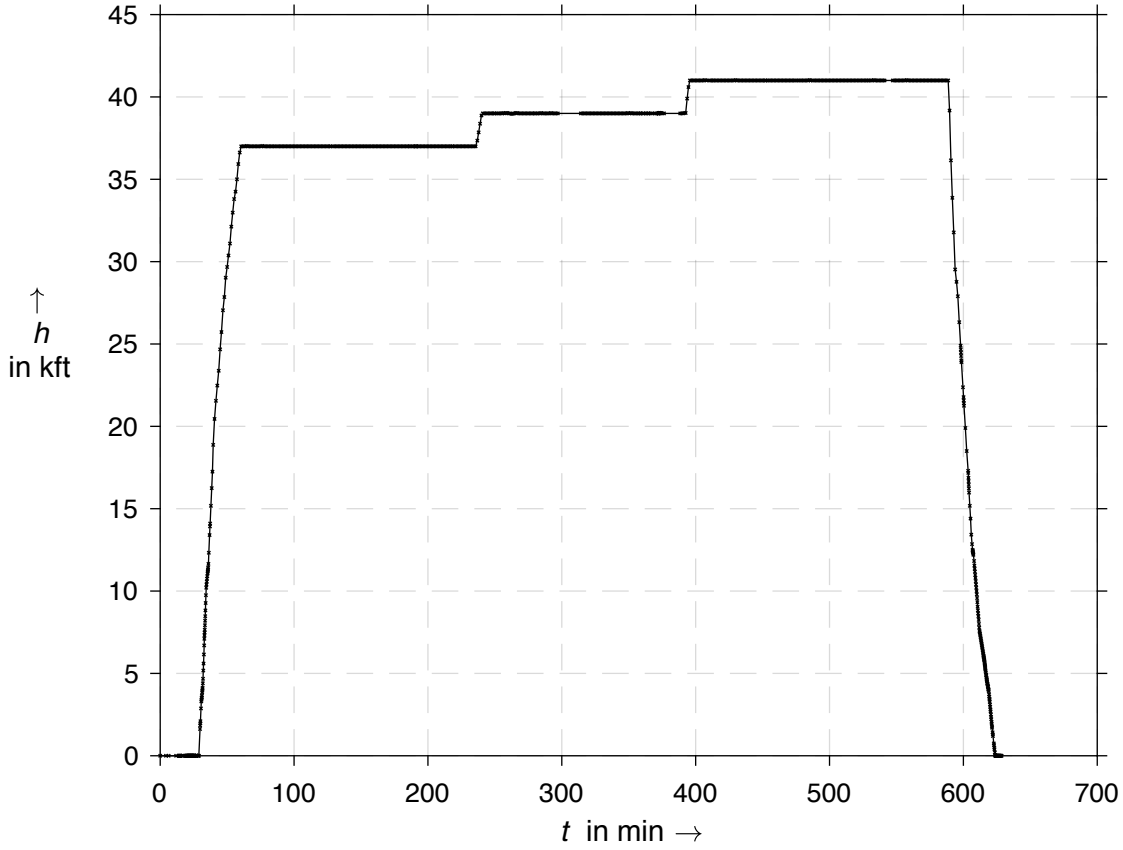

Figure 3.7 Altitude progression of an example flight from Frankfurt to Bangkok

t Time after first contact
h Altitude

In this case, the initial cruise altitude is 37,000 ft. During the flight, the aircraft performs two step climbs, to 39,000 ft at about 230 min and to 41,000 ft at about 395 min.

3.7 Discussion of the Cases

Examining the previous cases, it has been evaluated whether the data provided by Flightradar24 as a CSV download is suitable for further flight and aircraft performance analyses.

In some cases, the number of data points is not sufficient to issue accurate statements, so only estimations are possible. For these cases a high data rate is needed as specific parameters, like the ground speed during the take-off run, change quickly.

Further limitations occur due to the limited number of parameters included in the dataset. As only the ground speed is provided, it is challenging to derive the true airspeed because no wind information is available, as seen in the cruise flight case. In specific cases, like holding patterns, an estimation of the true airspeed is possible as ground speed information is available for several of different track angles in a short period. Therefore, variations in the true airspeed as well as in wind direction and velocity are minimized.

As the altitude information contained in the Flightradar24 data is related to a pressure of 1013.25 hPa, the flight level (FL) is given (**Skybrary 2020c**). Therefore, no statements about the geometric height can be issued.

Nevertheless, cases like determining the taxi time or the initial cruise altitude and step climbs show that the provided data can be used for further analyses if no high data rates are needed.

Although Flightradar24 also receives and processes additional data like true airspeed, GPS altitude and weather information (if available), this data is only visible for users holding a subscription plan. Further, this data is also not included in the CSV download files (see 3.1).

It should again be mentioned that to be able to perform an analysis, the flight to be analyzed needs to be inside Flightradar24’s coverage.

4 Initial Cruise Altitude and Step Climb Analysis

As could be seen in the previous Chapter, Flightradar24 data provided as a CSV download can be used best for macroscopic analyses not depending on high data rates nor speed information other than ground speed. Therefore, a more detailed study shall be conducted, mainly based on altitude data. In this Chapter, initial cruise altitudes and step climbs are investigated using a larger scale of data, also considering different aircraft types for comparison.

4.1 Breguet Range Equation

According to **Young 2001**, the still air range R for a turbofan-powered aircraft in level flight can be calculated using the true airspeed V, the glide ratio E, the specific fuel consumption c, the acceleration of free fall g and the mass m of the aircraft:

$$R = -\int_{m_{TO}}^{m_L} \frac{V\,E}{c\,g}\,\frac{1}{m}\,dm \tag{4.1}$$

Therein, m_{TO} is the aircraft's mass at take-off and m_L the aircraft's landing mass.

Several flight schedules, depending on the description of V and E during the cruise phase, are possible. A flight schedule with constant airspeed V and a constant lift coefficient c_L, and therefore constant E, is called cruise climb and leads to the Breguet Range Equation for obtaining the maximum range:

$$R = \frac{V\,E}{c\,g}\,ln\left(\frac{m_{TO}}{m_L}\right) \tag{4.2}$$

The lift coefficient c_L, taking into account lift L equals weight W in level flight conditions, can be written as:

$$c_L = \frac{L}{\frac{1}{2}\,\rho\,V^2\,S} = \frac{W}{\frac{1}{2}\,\rho\,V^2\,S} \tag{4.2}$$

The wing surface S remains the same throughout the cruise phase. The weight W of the aircraft decreases during the flight as fuel is consumed. To achieve a constant lift coefficient c_L at a constant airspeed V, the density ρ of the surrounding air needs to decrease.

This means the aircraft has to continuously gain altitude as the aircraft mass also decreases continuously. Due to air traffic control (ATC) restrictions, step climbs are performed instead of a continuous cruise climb.

Although Equation 4.1 is valid for level flight and the considered flight schedule demands the aircraft to climb, the deviation is neglectable due to the low climb angle. (**Young 2001**)

4.2 Data Acquisition

4.2.1 Flight Data

The fifteen wide-body passenger aircraft types with the most active aircraft and aircraft on order as of July 2019 (**Thisdell 2019**) have been used for this analysis. This accounts for more than 90 % of the wide-body fleet worldwide. In addition to that, five narrow-body aircraft types complement this analysis.

A total of 440 CSV files containing flight data have been downloaded from Flightradar24. As the CSV files only contain the Unix timestamp, UTC date and time information, callsign, position, altitude, ground speed and track (see 3.1), the aircraft type, as well as the IATA codes of the origin and destination airports, have been stored manually.

4.2.2 Airport Data

To be able to put the initial cruise altitude and step climbs in relation to the flight distance and the track, the coordinates of the origin and destination airports are needed. Here, the database provided in **Openflights 2020** is used. This database contains, among others, the IATA code, latitude, and longitude of more than 10,000 airports.

4.3 Data Preparation

To use the acquired data for this analysis, some preparations and calculations are made to provide additional information. The full dataset used for the analysis include:

- Aircraft type
- Great circle distance between origin and destination airport
- Track between origin and destination airport

- Initial cruise altitude and further cruise altitudes (if applicable)
- Altitude difference between two cruise altitudes
- Timestamp at which the cruise altitude is reached
- Time difference between two cruise altitudes
- Rate of climb during the step climb
- Flag indicating validity for initial cruise altitude analysis
- Flag indicating validity for step climb analysis

This data is stored in the spreadsheet *InitialCruiseAltitude_StepClimbs.xlsx* and is published on Harvard Dataverse. The download link can be found on page 2 of this project.

4.3.1 Distance between Origin and Destination Airport

The great circle distance between the origin airport and the destination airport is calculated using a MATLAB script provided by **Kleder 2019**. It calculates "the distance between points on the WGS-84 ellipsoidal Earth to a few millimeters of accuracy using Vincenty's algorithm" (**Kleder 2019**).

4.3.2 Track between Origin and Destination Airport

The track between the origin and destination airport is calculated using the *azimuth* function in MATLAB is used as described in **Matlab 2020a**.

4.3.3 Determination of Cruise Altitudes and Step Climbs

To determine the initial cruise altitude as well as the step climbs, the flight data is searched for level flights at a constant altitude that last for at least five minutes. The first level flight found above 19,500 ft is regarded as the initial cruise altitude. For the step climbs, steps with an increase in altitude of at least 100 ft compared to the previous cruise altitude are considered.

4.3.4 Detection and Handling of Flight Data Interruptions

As Flightradar24 does not provide worldwide flight tracking coverage (see 2.2), the downloaded flight data might be interrupted. A MATLAB script is used to determine whether interruptions in the flight data occur and whether these interruptions have an impact on the analysis of initial cruise altitudes and/or step climbs.

The script iterates through the flight data and checks whether the following conditions are met comparing two consecutive timestamps:

- time difference > 10 minutes
- altitude difference ≥ 50 ft

If both conditions are met, the current flight is not used for the analysis of step climbs. Flight data interruptions have also an impact on the analysis of initial cruise altitude if the conditions above occur before reaching the first level flight at a constant altitude for at least five minutes.

As climbs with a difference in altitude as low as 100 ft shall be considered, an altitude difference of 50 ft is applied in the condition to meet the restrictions due to the altitude resolution error of ±25 ft.

4.4 Analysis and Results

The number of analyzed flights per aircraft type as well as the validity information is presented in Table 4.1.

Table 4.1 Overview of analyzed flights per aircraft type

Aircraft Type	Total number of flights	No. of flights valid for step climb analysis	No. of flights valid for initial cruise altitude analysis
Airbus			
A220-100	20	20	20
A220-300	25	22	24
A320-200	11	10	11
A321-200	13	10	12
A330-200	18	10	15
A330-300	33	30	33
A330-900	11	10	10
A340-300	27	10	24
A340-600	16	10	16
A350-900	52	30	53
A350-1000	13	10	12
A380-800	12	11	12
Boeing			
B737-800	10	10	10
B747-400	11	10	11
B767-300	41	30	40
B777-200	13	10	13
B777-300	44	30	43
B787-8	14	10	13
B787-9	36	30	34
B787-10	10	10	10
Sum	**440**	**323**	**416**

For the following analyses in Chapters 4.4.1 and 4.4.2, at least ten data sets are provided for every aircraft type. For the analysis in Chapter 4.4.3 a minimum of 30 data sets per aircraft type have been considered.

4.4.1 Initial Cruise Altitude

Figure 4.1 to Figure 4.3 show the initial cruise altitudes relative to the great circle distance between the origin and the destination airport. Further, a linear regression helps to detect a tendency.

Figure 4.1 considers the five narrow-body aircraft types. For Airbus A220-100 and A220-300, it shows an increase in initial cruise altitude with the increase in great circle distance. The A320-200, A321-200 and Boeing 737-800 show a different behavior as the initial cruise altitude slightly decreases with an increase in great circle distance. Of these five, the Airbus A321-200 shows the steepest decline. The lowest initial cruise altitude is 21,000 ft (A220-300) with a distance of less than 300 km; the highest is 40,000 ft (A220-100 and A220-300) with a distance ranging between 1,500 km and 2,000 km.

The initial cruise altitudes of the Airbus wide-body aircraft types are depicted in Figure 4.2. All of them show a decreasing initial cruise altitude with increasing great circle distance. Of these aircraft types, the A330-300 shows the steepest and the A350-900 the gentlest decline. Here, the initial cruise altitudes range between 24,600 ft and 41,000 ft.

As for the Airbus wide-body aircraft types, the Boeing wide-body aircraft types in Figure 4.3 also show the same tendency. In this case, the Boeing 747-400 exhibits the steepest and the Boeing 767-300 the gentlest decline. Here, the initial cruise altitudes range between 28,000 ft and 41,000 ft.

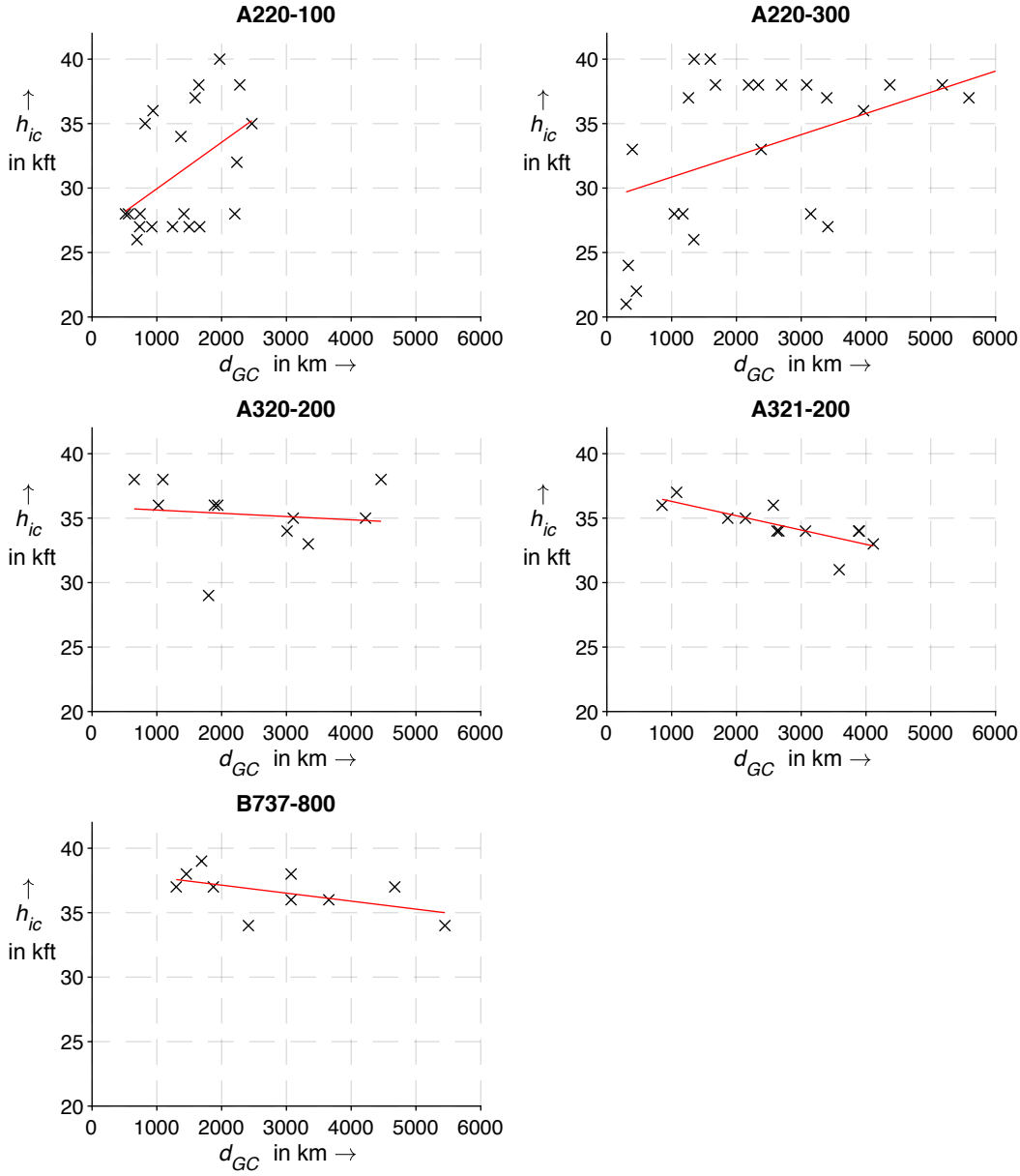

Figure 4.1 Initial cruise altitude relative to great circle distance of selected narrow-body aircraft types

d_{GC} Great circle distance between origin and destination airport
h_{ic} Initial cruise altitude
— Linear regression

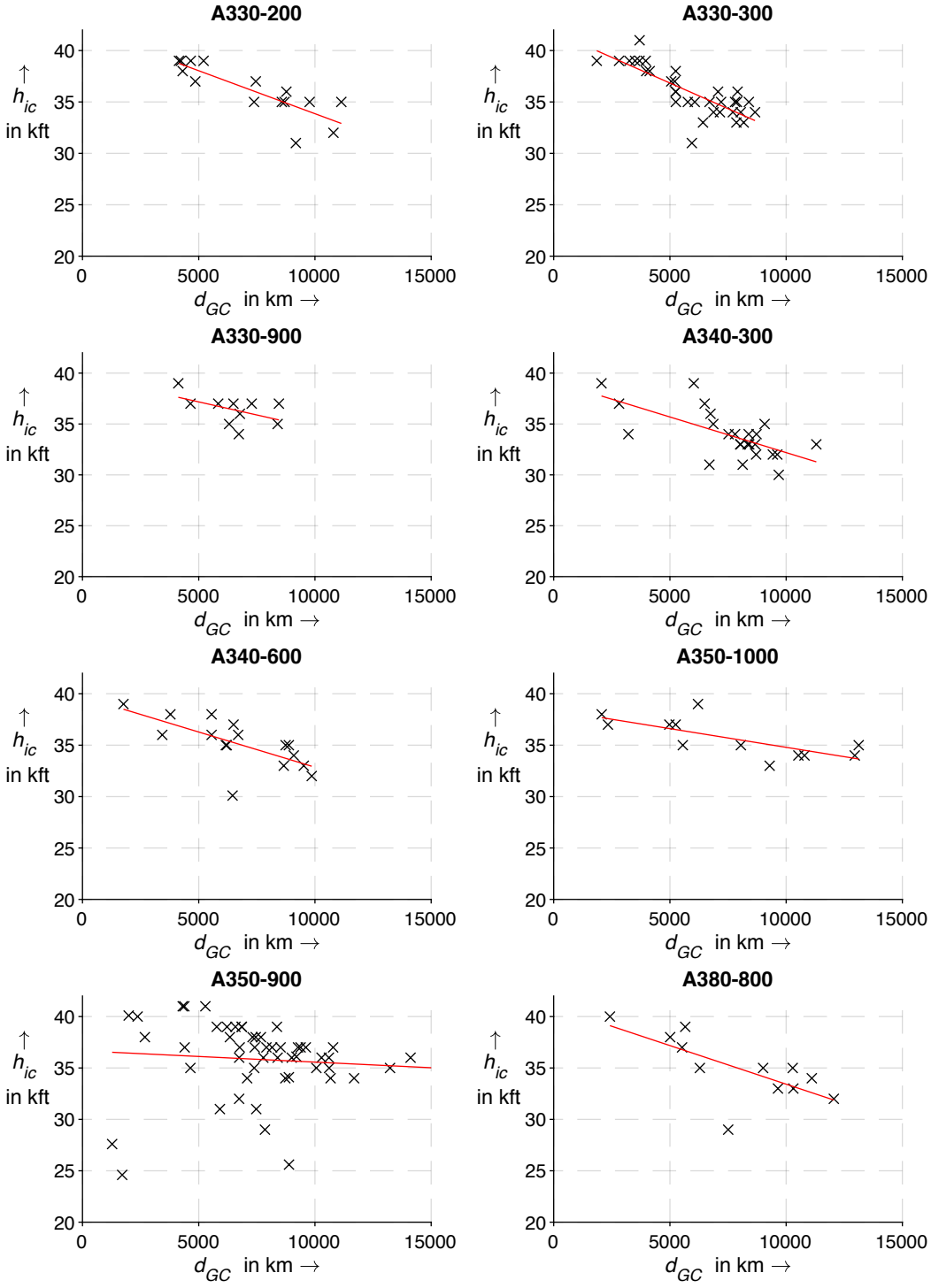

Figure 4.2 Initial cruise altitude relative to great circle distance of selected Airbus wide-body aircraft types

d_{GC} Great circle distance between origin and destination airport
h_{ic} Initial cruise altitude
— Linear regression

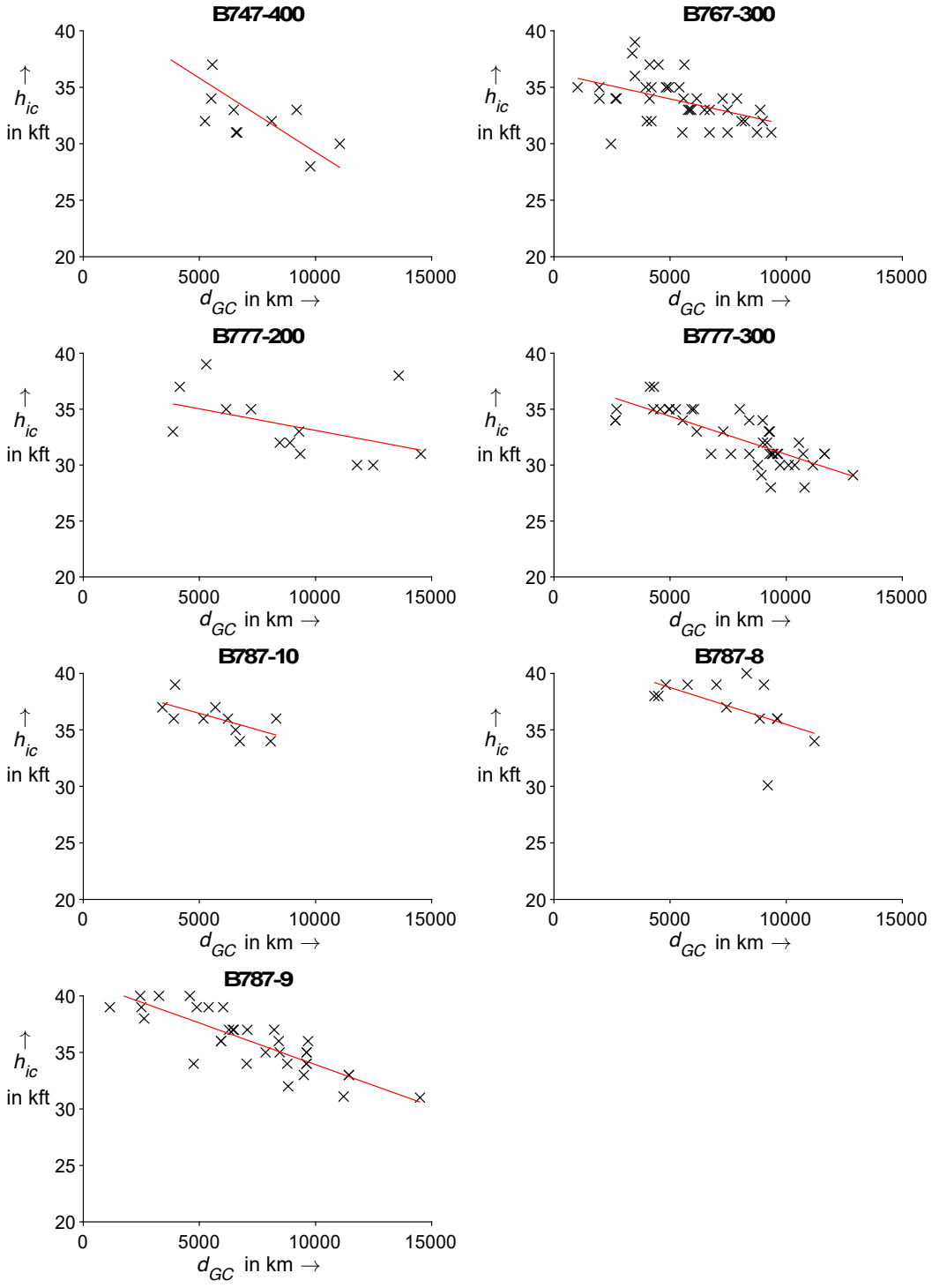

Figure 4.3 Initial cruising altitude relative to great circle distance of selected Boeing wide body aircraft types

d_{GC} Great circle distance between origin and destination airport
h_{ic} Initial cruising altitude
— Linear regression

4.4.2 Step Climbs

Figure 4.4 to Figure 4.6 show the number of step climbs relative to the great circle distance between the origin and the destination airport. Again, a linear regression depicts the tendencies.

For all of the narrow-body aircraft types, the number of step climbs increases with the great circle distance (Figure 4.4). In this case, the Boeing 737-800 exhibits the steepest and the Airbus A220-100 the gentlest increase. It can be observed that for most considered flights, no step climb has been performed during the cruise phase.

The Airbus wide-body aircraft types (Figure 4.5) as well as the Boeing wide-body aircraft types (Figure 4.6) also show an increase in step climbs with the great circle distance. Out of the flights considered, a maximum of five step climbs have been performed.

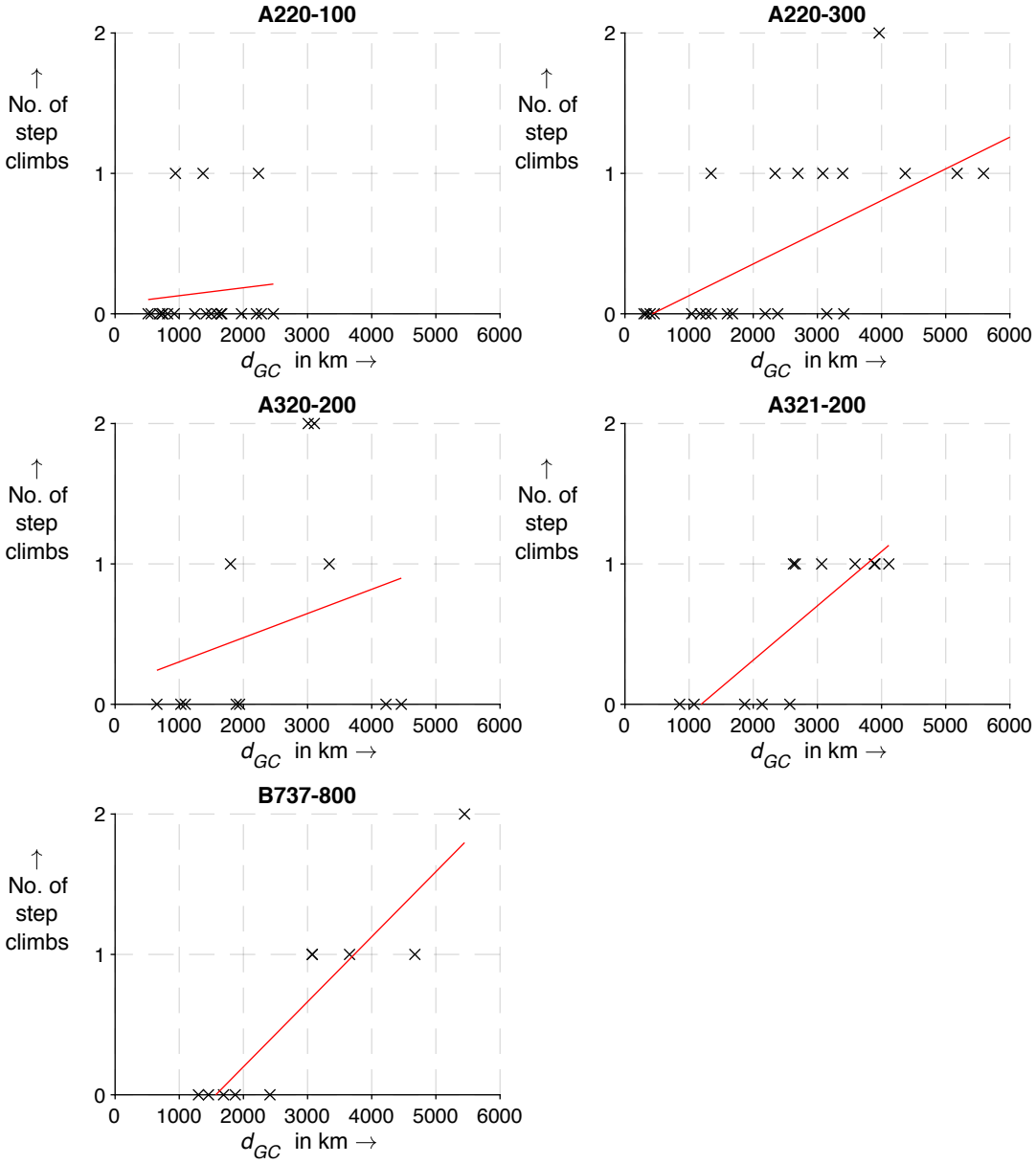

Figure 4.4 Number of step climbs relative to great circle distance of selected narrow-body aircraft types

d_{GC} Great circle distance between origin and destination airport

— Linear regression

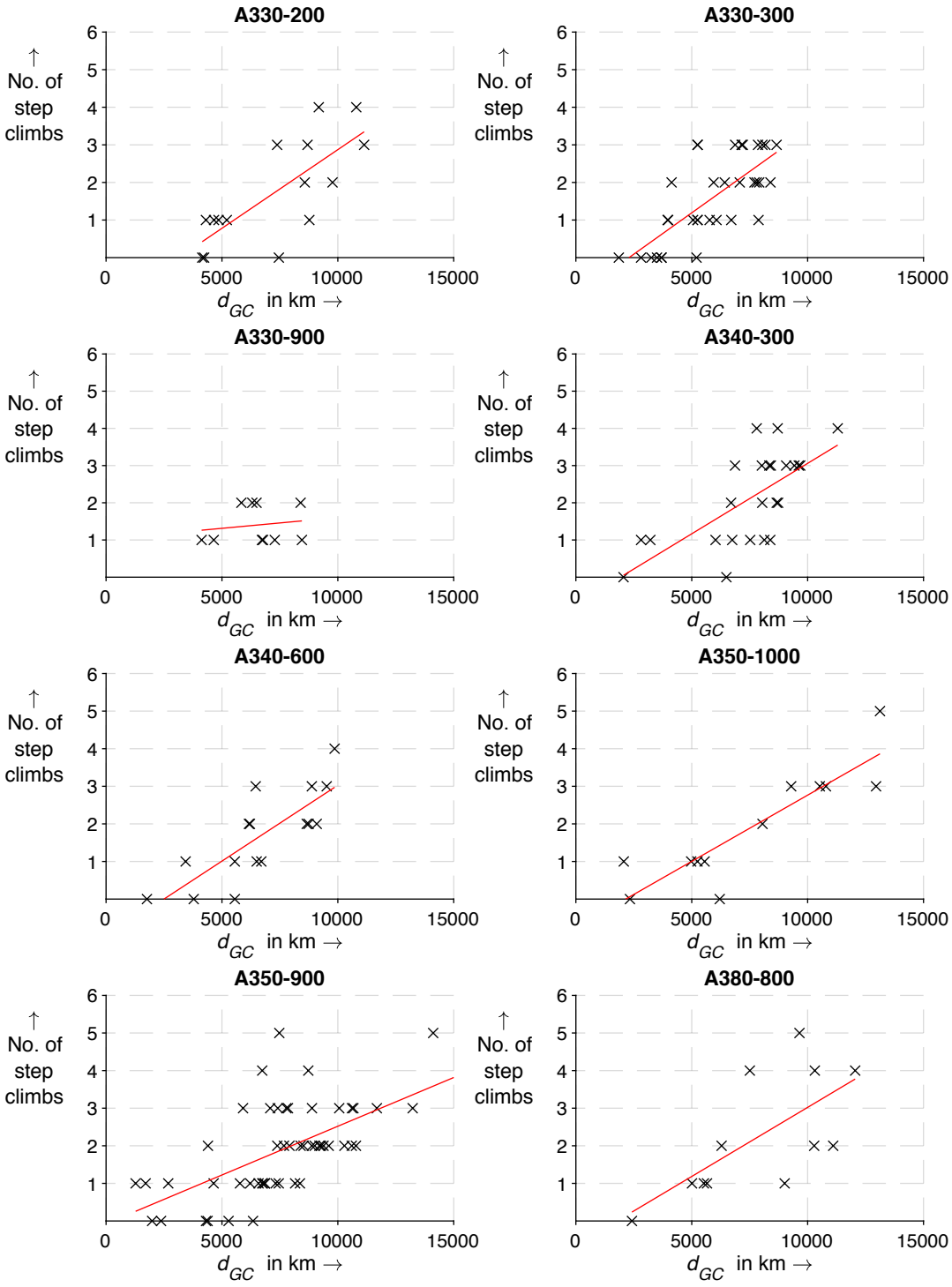

Figure 4.5 Number of step climbs relative to great circle distance of selected Airbus wide-body aircraft types

d_{GC} Great circle distance between origin and destination airport

Linear regression

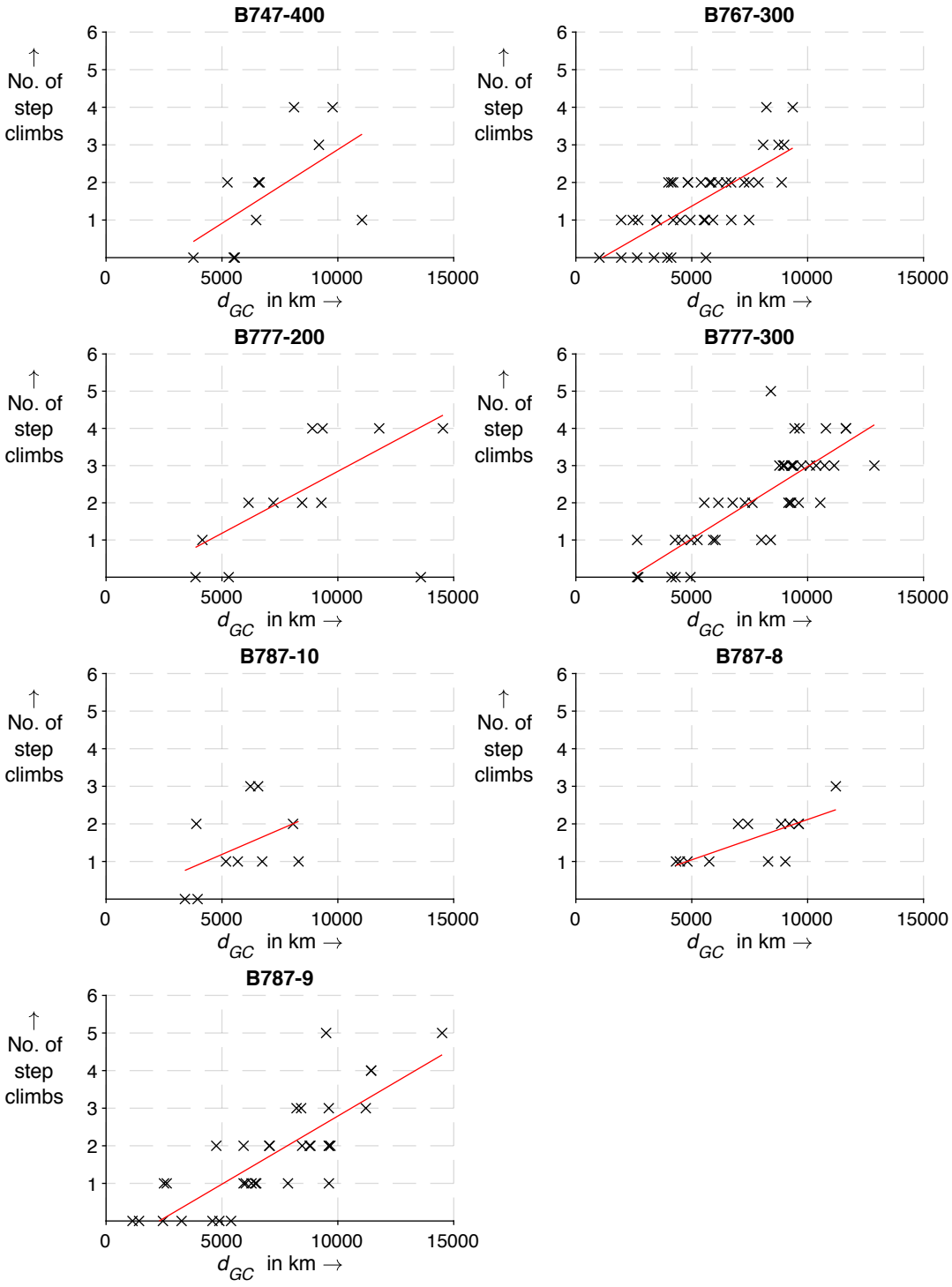

Figure 4.6 Number of step climbs relative to great circle distance of selected Boeing wide-body aircraft types

d_{GC} Great circle distance between origin and destination airport

— Linear regression

4.4.3 Wide-body Aircraft Type Statistics

Following the more general analysis of initial cruise altitude and step climbs, a more detailed analysis of the five most common wide-body aircraft types is conducted. For these aircraft types at least 30 flight data sets are available to provide a larger sample size.

Box plots are used to depict various statistical values in a compact manner. The horizontal red line shows the median while the blue box indicates the first and third quartile. Black whiskers are used to show the range of values that are not considered outliers. The red pluses mark outliers, i. e. their value is lower or greater than 2.7 σ of the sample data. (**Matlab 2020b**)

Figure 4.7 shows the box plots for the number of step climbs per 1000 km for the five wide-body aircraft types. One can see that the medians range between approx. 0.35 and 0.45. Further, several outliers can be observed, especially in the case of the A350-900. Here, the highest ratio is nearly 1.6 steps per 1000 km.

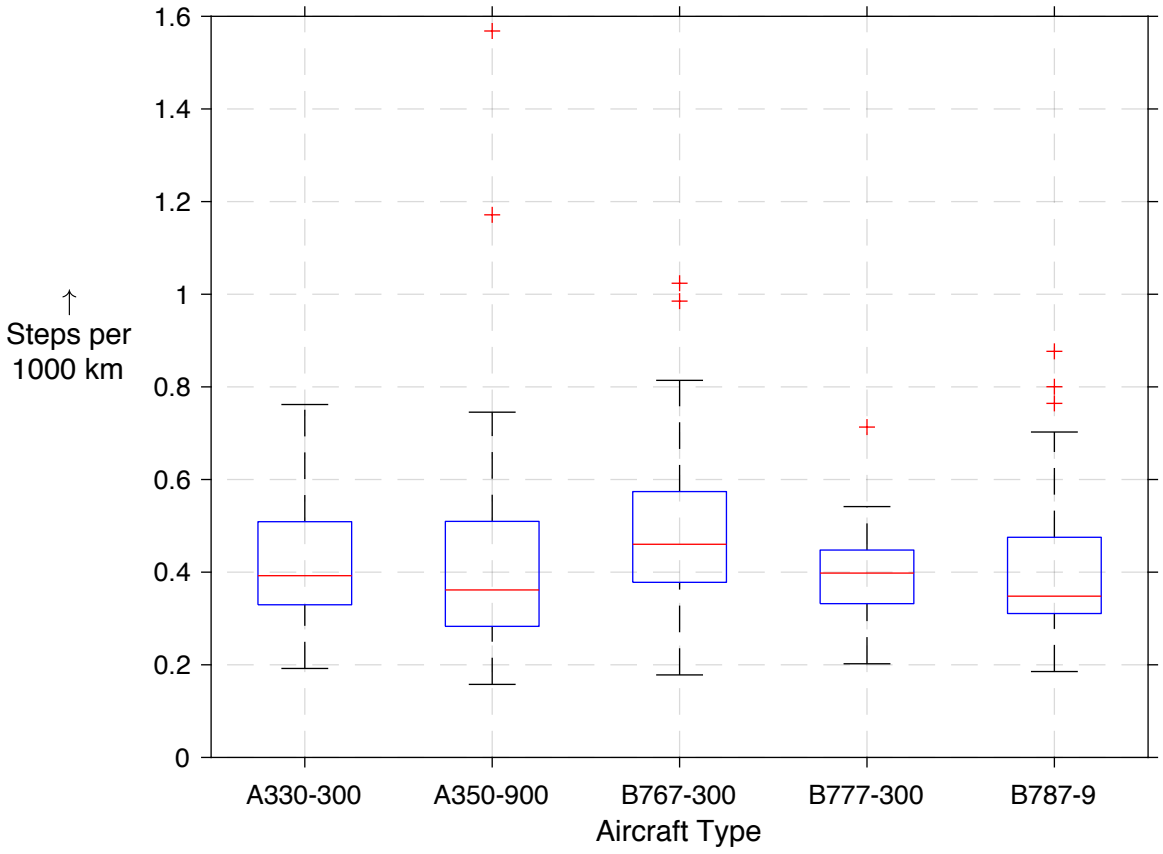

Figure 4.7 Number of step climbs per 1000 km

The differences in altitude during the step climbs are depicted in Figure 4.8. It clearly shows that the majority of step climbs exhibit an increase in altitude of 2000 ft. The outliers range between 100 ft and 4000 ft for Airbus A330-300, Boeing 767-300, 777-300 and 787-9 but reach almost 14,000 ft for the Airbus A350-900.

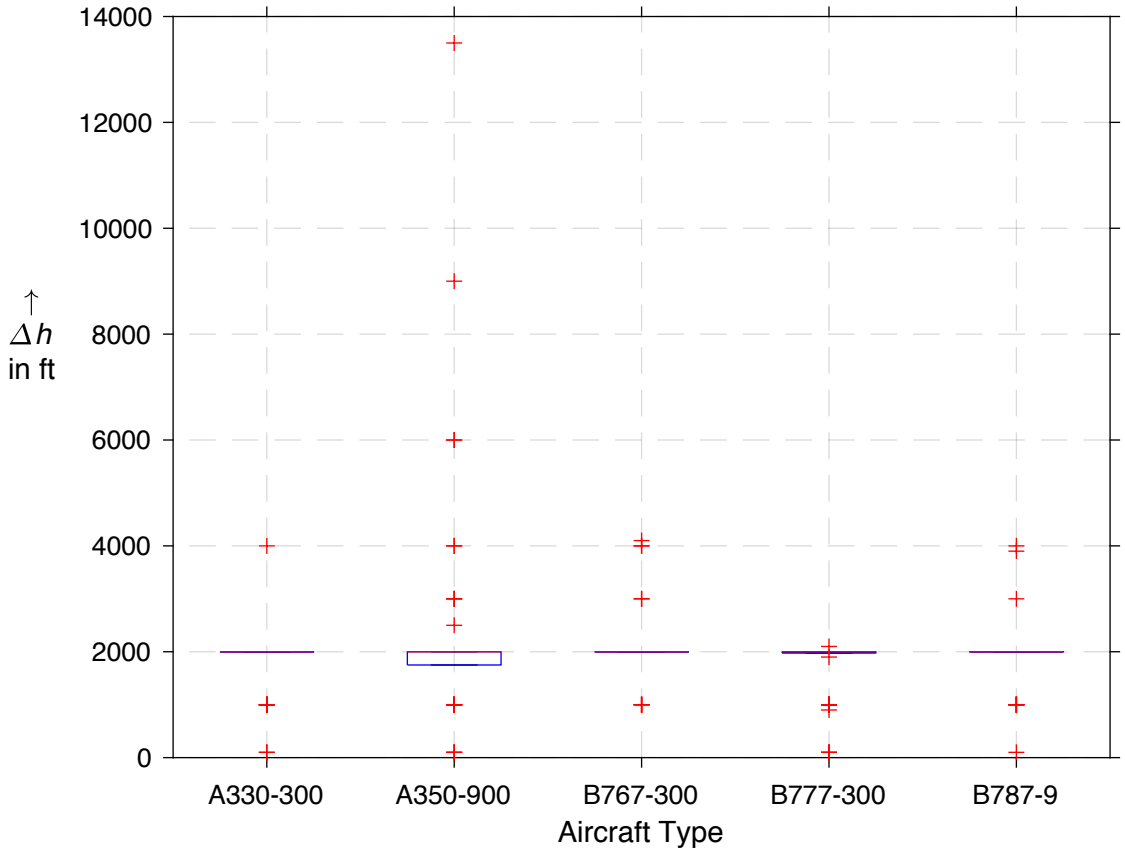

Figure 4.8 Altitude difference during step climb

Δh Altitude difference during step climb

Figure 4.9 presents the time between step climbs. The medians range between 100 and 150 minutes. It can also be observed that the time difference ranges between about 10 and 400 minutes without showing any outliers.

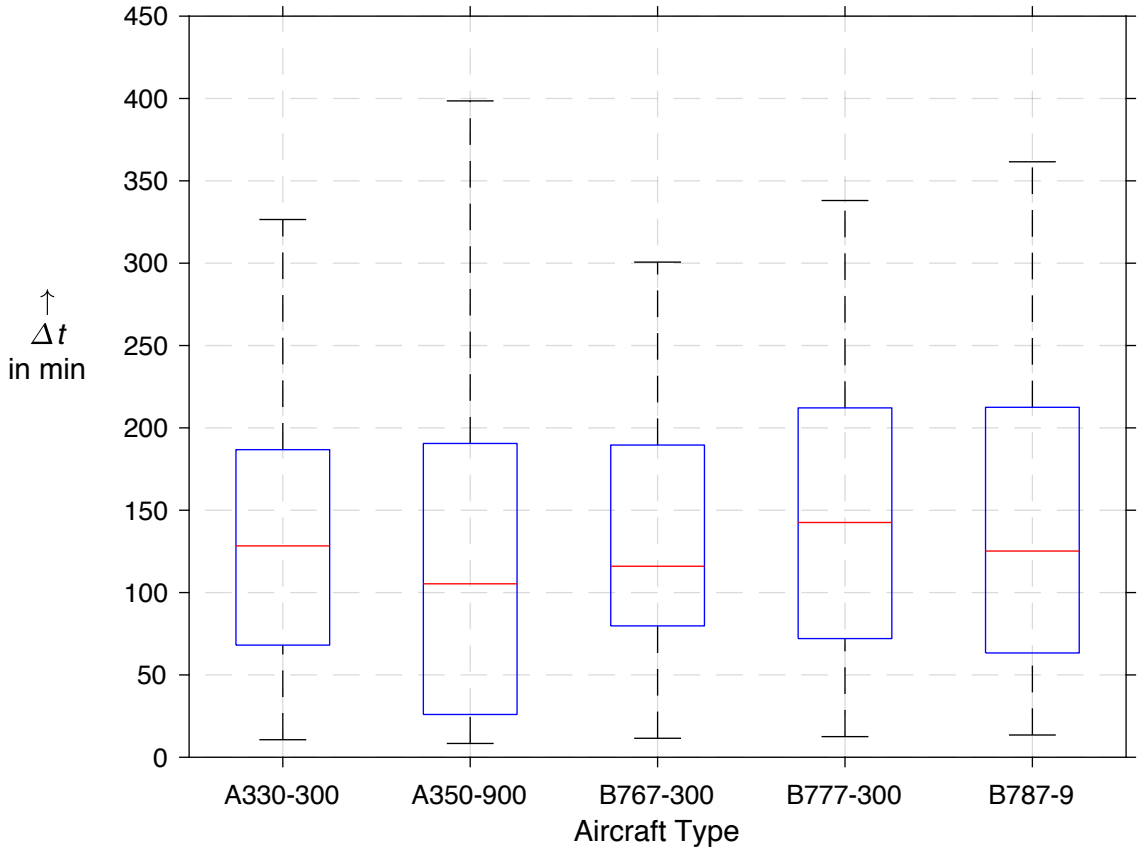

Figure 4.9 Time between step climbs

Δt Time difference between two step climbs

Figure 4.10 shows the rate of climb during the step climbs, calculated as the quotient of altitude difference and time difference. In this case, the medians range between 450 and 650 ft/min. As seen before, the whiskers describe a wide range of values. Again, several outliers exist.

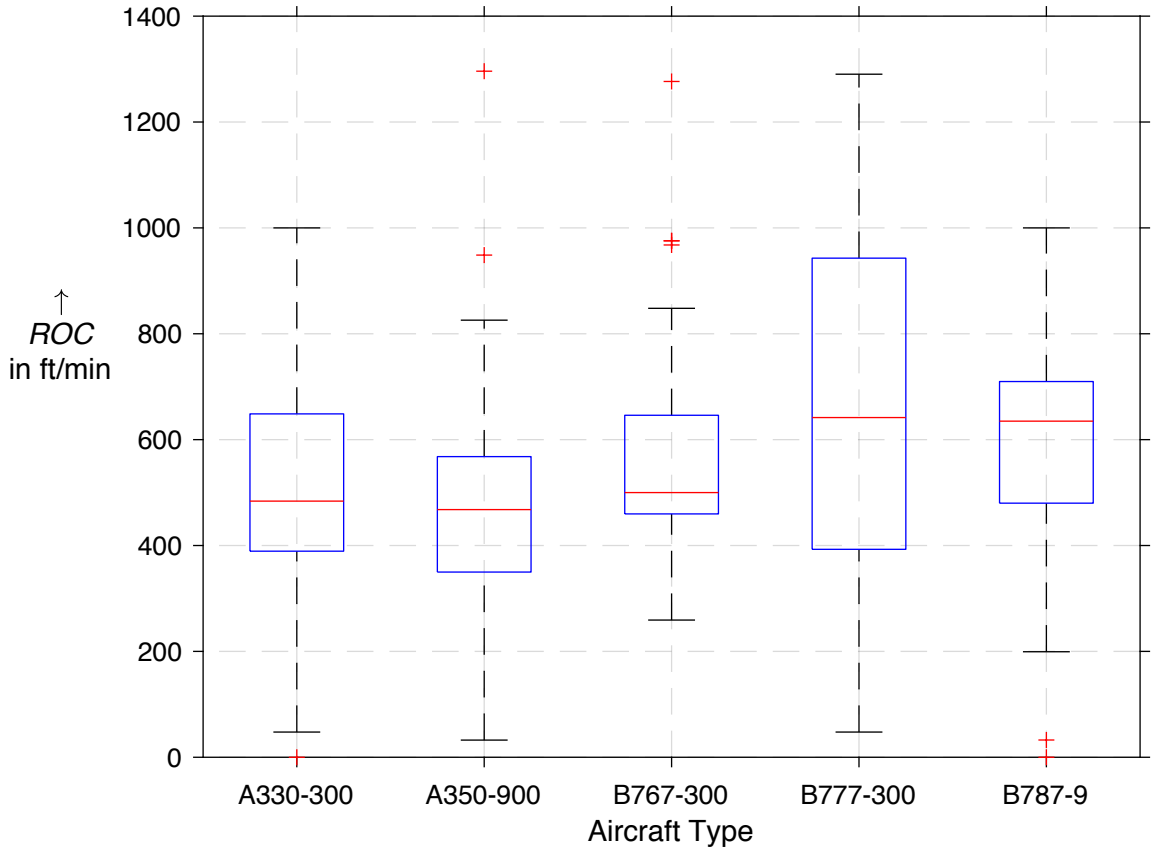

Figure 4.10 Vertical speed during step climbs

ROC Vertical speed

4.4.4 Cruise Altitudes

Figure 4.11 shows all cruise altitudes of all considered flights relative to the track (azimuth) between the origin and the destination airport.

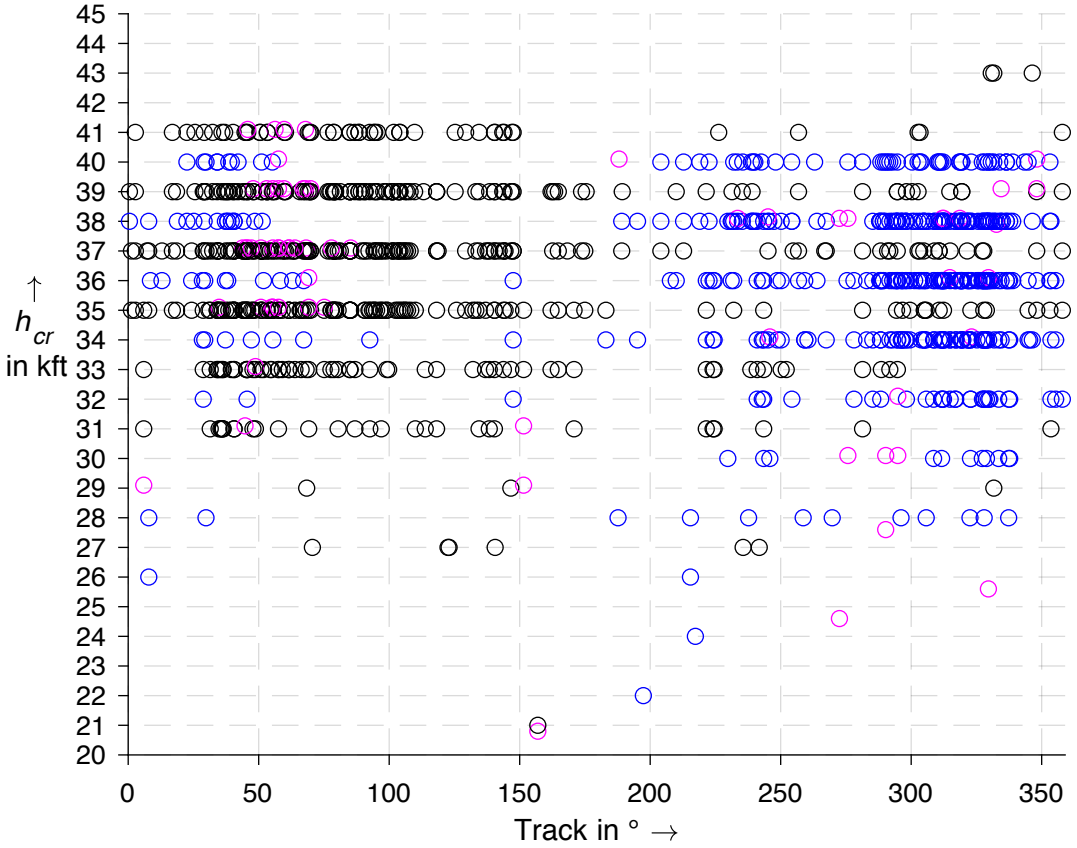

Figure 4.11 Cruise altitudes related to the track between origin and destination airport

Track	Track between origin and destination airport
h_{cr}	Cruise altitude
○	Even flight levels
○	Odd flight levels
○	Neither even nor odd flight levels

It can be seen that there is a concentration of odd flight levels among flights in eastern direction and a concentration of even flight levels among flights in western direction. This relates to **ICAO 2005** which specifies odd flight levels for a flight direction between 0° and 179° as well as even flight levels for a flight direction between 180° and 359° (magnetic heading). This also explains why the median of altitude differences of step climbs is 2000 ft and only shows little variation (Figure 4.8). Up to an altitude of 41,000 ft, a vertical separation of 1000 ft between flight levels is applied. In some regions, where a reduced vertical separation minimum (RVSM) is not implemented, a vertical separation of 2,000 ft applies between 29,000 ft and 41,000 ft. (**ICAO 2005**)

Further, several cruise altitudes can be observed that represent neither odd nor even flight levels. This applies in “areas where metres are the primary unit of measurement for altitude” (**ICAO 2005**), like in Chinese airspace. This can explain the outliers in Figure 4.8, especially those at 100 ft and 600 ft. They are a common altitude adjustment when entering Chinese airspace between altitudes of 22,000 ft and 41,000 ft.

4.5 Discussion of the Analysis

Regarding the 20 considered aircraft types, most of them show the tendency of a lower initial cruise altitude at greater flight distances. Further, the number of steps increases with flight distance. Only the Airbus A220-100 and A220-300 show a different behavior as the initial cruise altitude increases with the flight distance.

It can also be observed that, in both cases, the gradients of the linear regressions differ between the aircraft types. Due to the limited number of samples per aircraft type and the partly high spread, it is difficult to derive characteristics for the different types.

Additionally, it is not possible to make an accurate statement on the minimum flight distance at which a step climb is performed. For the narrow-body aircraft types, a step climb could be observed as early as at a flight distance below 500 km. At the same time, another flight with a distance of about 4,500 km remained on the same flight level for its entire cruise phase.

The statistics considering only the five most common wide-body aircraft types can provide an indication for the analyzed parameters, but, except the altitude difference, the values, again, show a high spread.

It is not clear whether these differences come from flight- and route-specific influences or from actual aircraft type dissimilarities. To better detect and understand the differences between the aircraft types, it requires larger sample sizes.

The calculation of the rate of climb (ROC) is flawed due to the sometimes-low data rate. This can lead to a lower rate of climb as a longer time frame has been considered for calculation than the actual step climb phase endured.

Besides, altitude adjustments can have several reasons. This could be for instance due to the change of airspace with different rules (as seen in Chapter 4.4.4) or weather conditions. It does not necessarily need to be a step climb as described in Chapter 4.1. Whether the step climb was requested by the pilots or the change in altitude was demanded by the air traffic controller remains unknown. Further, step climb intentions by the pilots could also have been denied by the air traffic controller, possibly due to traffic reasons on that route. Including this aspect in the analysis, potential links between step climbs and air traffic could lead to a better understanding.

It should also be mentioned that descends during the cruise phase have not been considered in this study.

Nonetheless, this study gives an example and proves that Flightradar24 data is in general suitable for macroscopic flight analyses, especially considering the whole cruise phase of flights worldwide.

5 ADS-B and Extended Mode S Data

Mode S is a secondary surveillance radar (SSR) interrogation mode and enables selective communication with individual aircraft. This advantage over the older Mode A and C technology is achieved by the allocation of a unique 24-bit address to an aircraft. Furthermore, Mode S allows the transmission of more data compared to Mode A and C which is only capable of reporting the identity as well as the barometric pressure altitude of an aircraft. (**Skybrary 2020d**)

ADS-B stands for automated dependent surveillance-broadcast and is a surveillance technology based on the aircraft transmitting its precise location and other data without the need for interrogations. It is automated because no external interrogation is needed and dependent because it depends on onboard equipment. The position information is primarily provided by a global navigation satellite system (GNSS). (**EASA 2018b**) As a datalink technology for ADS-B, Universal Access Transceiver (UAT) and the Mode S 1090 MHz Extended Squitter (1090ES) technology can be used. The latter is the most common technology. (**Skybrary 2020a**)

The Mode S transponder provides several downlink formats (DF) which are used for different tasks. Table 5.1 gives an overview of the most important downlink formats for receiving ADS-B and Extended Mode S messages.

Table 5.1 Downlink Format Overview (adapted from **EASA CS-ACNS**)

Downlink Format	Description
17	1090ES (ADS-B)
20	Comm-B reply (altitude reply)
21	Comm-B reply (identity reply)

Downlink format DF17 is used for ADS-B messages from Mode S transponders. The downlink formats DF20 and DF21 are both used for Comm-B replies containing the data of the requested register (see 5.2). In addition to that, DF20 provides altitude information while DF21 provides the Mode A code. (**EASA CS-ACNS**)

5.1 ADS-B Message Types

The preamble of ADS-B messages contains, among others, the downlink format, the type code of the message and the 24-bit ICAO address of the ADS-B participant. The content of the data frame depends on the ADS-B message type. Table 5.2 gives an overview of the different message types, each type providing different information about the aircraft.

Table 5.2 ADS-B Message Types (DF 17) (adapted from **EASA CS-ACNS**)

Type Code	ADS-B Message Type
1-4	Aircraft identification and category (AICM)
5-8	Surface position (SPM)
9-18	Airborne position (APM)
19	Airborne velocity (AVM)
20-22	Airborne position (APM)
23	Test message
24-27	Reserved
28	Aircraft status
29	Target state and status (TSSM)
30	Reserved
31	Aircraft operational status (AOSM)

The data frames are stored in different registers. The Mode S transponder has 256 registers which can be addressed by Comm-B data selectors (BDS). Table 5.3 shows the different ADS-B message types, their corresponding BDS code, the parameters stored in this register as well as the resolution of the parameter values. It should be noted that not all of the parameters are mandatory for ADS-B operation. (**EASA CS-ACNS**)

Table 5.3 ADS-B messages and corresponding parameters (adapted from **EASA CS-ACNS** and **ICAO 9871**)

ADS-B message type	BDS code / register	Parameters	Resolution
Airborne position	0,5	Barometric altitude[a]	25 ft
		GNSS height[b] (height above ellipsoid)	25 ft
		Latitude (CPR format[c])	-
		Longitude (CPR format)	-
Surface position	0,6	Ground speed	0.125 kt – 5.0 kt
		True ground track	2.8125°
		Latitude (CPR format)	-
		Longitude (CPR format)	-
Aircraft identification and category	0,8	Aircraft category (used for wake vortex characteristics)	-
		Callsign or registration	-
Airborne velocity	0,9	Ground speed[d] (east-west and north-south velocities are transmitted separately)	1 kt[e] – 4 kt[f]
		Vertical rate (either from barometric or geometric source)	64 ft/min
		Difference between geometric height and barometric altitude[d]	25 ft
		Airspeed[g] (TAS or IAS)	1 kt[e] – 4 kt[f]
		Magnetic heading[g]	0.3515625°
		Track[h] (true north)	-
Aircraft status	6,1	Emergency/Priority status, TCAS RA broadcast	-
Target state and status	6,2	Selected altitude (MCP/FCU or FMS)	32 ft
		Barometric pressure setting	0.8 mbar
		Selected heading	0.703125°
		Autopilot status	-
		VNAV mode status	-
		Altitude hold mode status	-
		Approach mode status	-
		TCAS operational status	-
Aircraft operational status	6,5	Operational information and capabilities of ATC-related applications	-

[a] type codes 9 to 18

[b] type codes 20 to 22

[c] compact position reporting requires two position messages (odd and even) or a reference position near the current aircraft position to unambiguously determine the position of the aircraft

[d] only subtype codes 1 and 2

[e] normal flight conditions

[f] supersonic flight conditions

[g] only subtype codes 3 and 4

[h] true track can be derived from the east-west and north-south velocity components

Not all ADS-B messages are broadcast periodically as the aircraft status message is only broadcast when triggered. Table 5.4 shows the broadcast rates for the different ADS-B messages.

Table 5.4 Broadcast rates of ADS-B messages in airborne state (adapted from **ICAO 9871**)

ADS-B message type	Broadcast rate in messages/second	Broadcast type
Airborne position	2	periodic
Airborne velocity	2	periodic
Aircraft identification and category	0.2	periodic
Aircraft status	0.19 – 1.43	event-driven
Target state and status	0,77 – 0,83	periodic
Aircraft operational status	0,38 – 1,43	periodic

5.2 Comm-B Replies

Other than ADS-B messages, Comm-B messages are the replies to specific interrogations via Uplink by an ATC ground station. Its purpose is to provide additional information about the aircraft and flight data to ATC. As the ground station knows what message to expect, no indication of the message type is transmitted in the signal.

In Europe, Mode S has been introduced in two stages. The first stage, Mode S Elementary Surveillance (ELS), provides basic information about the transponder capabilities and aircraft identification. A full list of the Comm-B replies considered in ELS can be found in Table 5.5, together with their BDS code and the parameters contained therein.

Table 5.5 Comm-B messages and corresponding parameters or information (ELS) (adapted from **EASA CS-ACNS**)

Comm-B message	BDS code / register	Parameters/information
Data link capability report	1,0	Information on data link capability of the airborne surveillance system
Common usage GICB capability report	1,7	Information on additional services available
Aircraft identification	2,0	Callsign or aircraft registration
ACAS active resolution advisory	3,0	Resolution advisories (RAs) report

The second stage, Mode S Enhanced Surveillance (EHS), makes use of downlinked aircraft parameters which provide more information about the aircraft and the flight state. Table 5.6 gives an overview of the Comm-B replies considered in EHS.

Table 5.6 Comm-B messages and corresponding parameters (EHS) (adapted from **EASA CS-ACNS** and **ICAO 9871**)

Comm-B message (register assignment)	BDS code / register	Parameters	Resolution
Selected vertical intention	4,0	MCP/FCU selected altitude	16 ft
		FMS selected altitude	16 ft
		Barometric pressure setting	0.1 mbar
		MCP/FCU mode (VNAV mode, Altitude hold mode, Approach mode)	-
		Target altitude source	-
Track and turn report	5,0	Roll angle	0.17578125°
		True track angle	0.17578125°
		Ground speed	2 kt
		Track angle rate	0.03125°/s
		True airspeed	2 kt
Heading and speed report	6,0	Magnetic heading	0.17578125°
		Indicated airspeed	1 kt
		Mach number	0.004
		Barometric altitude rate	32 ft/min
		Inertial vertical velocity	32 ft/min

Besides, there are other registers containing information about the aircraft state as well as the environment which are neither part of ELS nor EHS. Three of them, containing valuable information regarding aircraft performance, are listed in Table 5.7.

Table 5.7 Comm-B messages and corresponding parameters (other registers) (adapted from **EASA CS-ACNS** and **ICAO 9871**)

Comm-B message (register assignment)	BDS code / register	Parameters	Resolution
Meteorological routine air report	4,4	Wind speed	1 kt
		Wind direction (true)	0.703125°
		Static air temperature	0.25 °C
		Average static pressure	1 hPa
		Turbulence[a]	-
Meteorological hazard report	4,5	Turbulence[a]	-
		Wind shear[a]	-
		Microburst[a]	-
		Icing[a]	-
		Wake vortex[a]	-
		Static air temperature	0.25 °C
		Average static pressure	1 hPa
		Radio height	16 ft
Air-referenced state vector	5,3	Magnetic heading	0.17578125°
		Indicated airspeed	1 kt
		Mach number	0.008
		True airspeed	0.5 kt
		Altitude rate	64 ft/min

[a] possible category: nil, light, moderate, severe

5.3 Receiving Equipment

5.3.1 Receiver Hardware

The following hardware is used for the homebuilt ADS-B and Mode S receiver:

- FlightAware Pro Stick Plus (USB software defined radio with built-in amplifier, 1090 MHz filter and connector for antenna)
- DVB-T antenna, customized for 1090 MHz operation
- Raspberry Pi 2 Model B

5.3.2 Decoding Software

The decoding software dump1090 is used to feed the received raw data to a transmission control protocol (TCP) port. This raw data is then checked for errors and stored in a CSV file using a python script based on the library pyModeS as described in **Sun 2019**. The file contains, besides the raw message, the timestamp, the ICAO 24bit-address, the downlink format and the type code (ADS-B messages) or the most probable BDS code (Comm-B replies). The decoding of the raw ADS-B and Mode S messages is realized by another python script which is also based on the library pyModeS. This script is able to filter for a specific ICAO 24bit-address, decode the messages and to store this data in CSV files, sorted according to message types.

It should be mentioned that not all parameters and information as described in Chapters 5.1 and 5.2 can be decoded using the present script, especially those stored in registers 1,0 (Data link capability report), 3,0 (ACAS active resolution advisory), 6,1 (Aircraft status) and 6,5 (Aircraft operational status).

Both python scripts, *ADS-B_ModeS_Feed_to_CSV.py* for evaluating and storing the raw messages to a CSV file and *ADS-B_ModeS_Decoder.py* for the decoding of the messages, are published on Harvard Dataverse. The download link can be found on page 2 of this project.

5.4 Example Data

As an example, the ADS-B and Extended Mode S data of flight UAL961 from Frankfurt/Main (FRA/EDDF) to Newark (EWR/KEWR) operated by a Boeing 787-10 on 28th December 2019 has been recorded using the homebuilt receiver set-up. Further, this data has been decoded and analyzed.

The full data set is stored in the spreadsheet *A05629_ADS-B_Mode_S.xlsx* and is published on Harvard Dataverse. The download link can be found on page 2 of this project.

The first message from the example flight was received at 1577529842.8867211 and the last message at 1577530558.39862 (Unix time). During this time of approx. 11 minutes and 56 seconds, a total of 3,487 messages has been received. This means, on average, approx. 4.87 messages have been received per second. 1,758 of those are ADS-B messages and 1721 are Comm-B replies. The breakdown of the ADS-B message types can be found in Table 5.8.

Table 5.8 Breakdown of received ADS-B messages

Message type	Total number of messages received	Average receiving rate in messages/second
Surface position	0	0
Airborne position	670	0.94
Airborne velocity	616	0.86
Aircraft identification and category	62	0.09
Aircraft status	56	0.08
Target state status	244	0.34
Aircraft operational status	110	0.15

No surface position message has been received as the first message was received when the aircraft has already been airborne. The breakdown of the received Comm-B replies can be found in Table 5.9.

Table 5.9 Breakdown of received Comm-B messages

Comm-B Message Type	Total number of messages received	Average receiving rate in messages/second
Data link capability report	32	0.04
Common usage GICB capability report	48	0.07
Aircraft identification	107	0.15
ACAS active resolution advisory	0	0
Selected vertical intention	635	0.89
Track and turn report	245	0.34
Heading and speed report	654	0.91
Meteorological routine air report	0	0
Meteorological hazard report	0	0
Air-referenced state	0	0

Of the 1,721 Comm-B replies, 1,366 messages were sent with DF20 containing altitude information and 355 messages with DF21 containing Mode A code. In the case of 158 Comm-B messages, the decoding software could not unambiguously determine the message type and manual processing was needed. This amounts to approx. 9.1 % of all received Comm-B messages.

No meteorological routine air report, meteorological hazard report or air-referenced state messages have been received because the transponder of the aircraft does not show capability (see BDS code 1,7) for these BDS codes. The remaining eight messages did not contain any data.

The following information about the aircraft/flight does not change throughout the flight:

- Aircraft ICAO 24bit address: A05629
- Callsign: UAL961
- Aircraft category: 5
- ADS-B version: 2

- Supported BDS codes: 05, 06, 07, 08, 09, 0A, 20, 21, 40, 50, 51, 52, 5F, 60

Figure 5.1 shows the flight path of the example flight relative to the location of the origin airport and the receiver location. The airborne position message provides the position information. The maximum distance from the aircraft to the receiver location amounts to approx. 85 km.

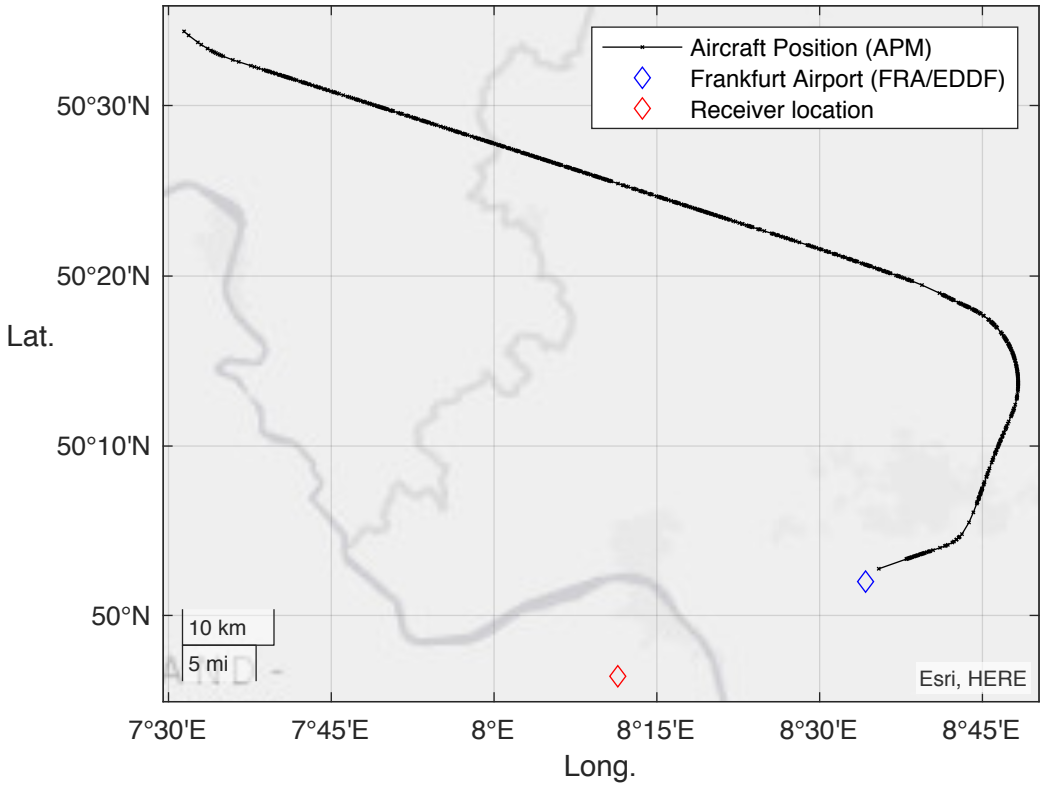

Figure 5.1 Aircraft flight path in relation to origin airport and receiver location

The progression of the barometric altitude, the selected heading and the difference between the geometric height and the barometric altitude can be found in Figure 5.2. One can see that the selected altitude on the mode control panel (MCP) or flight control unit (FCU) is raised before the aircraft reaches the set altitude so that a continuous climb is possible.

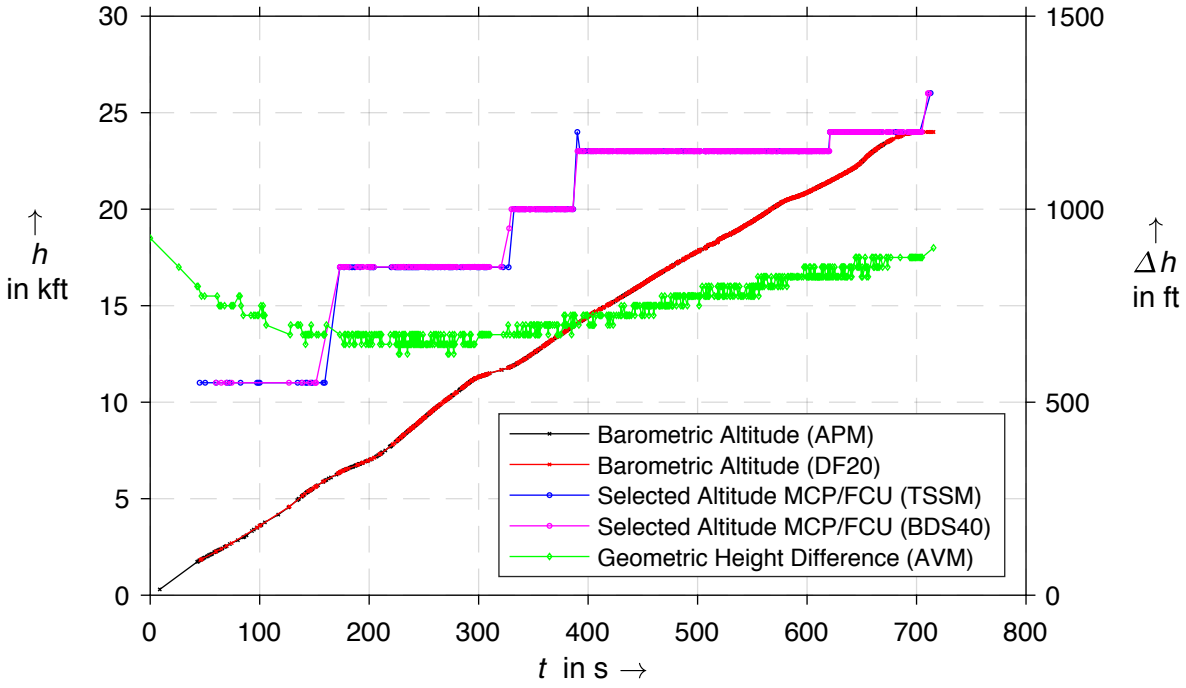

Figure 5.2 Altitude information

t	Time after first contact
h	Altitude
Δh	Altitude difference between Geometric Height and Barometric Altitude

Figure 5.3 shows the barometric pressure setting. The pressure was set from approx. 1041 hPa to the standard pressure of 1013.25 hPa after about 120 s after the first contact with the aircraft. Taking a look at the progression of the barometric altitude in Figure 5.3, one can see that this happened at a barometric altitude of approx. 5,000 ft which is the transition altitude (TA) at Frankfurt/Main airport. (**IVAO 2020**) At this altitude, the barometric pressure has to be set to the standard pressure of 1013.25 hPa, so that all aircraft in an area with the same air pressure use the same reference and therefore keep the needed vertical separation.

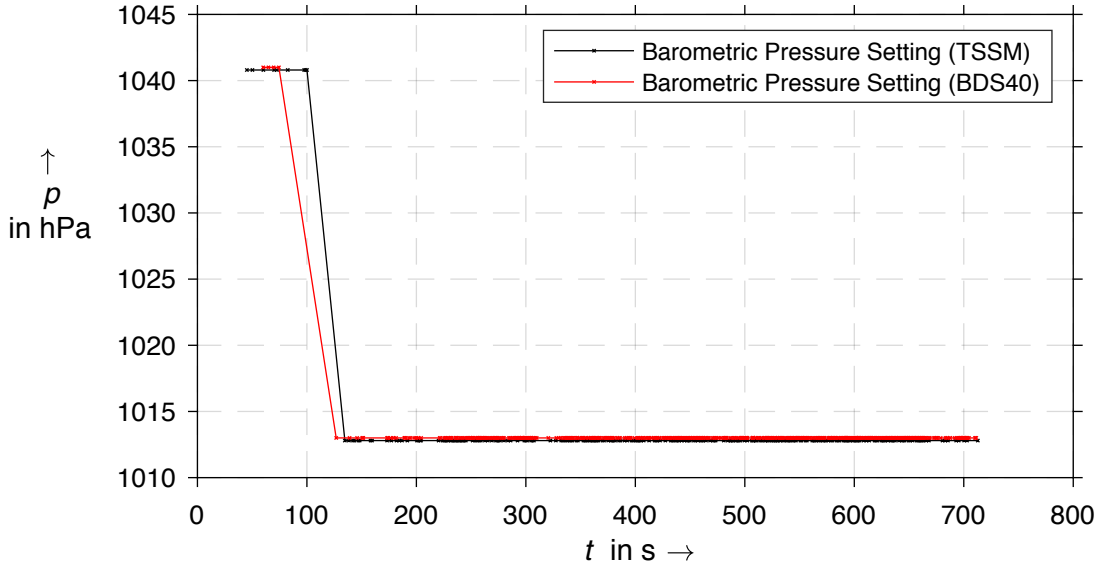

Figure 5.3 Barometric pressure setting

t	Time since first contact
p	Pressure

Figure 5.4 shows the vertical rate of the aircraft provided by different sources. One can see that although all three show the same progression, the vertical rate derived from barometer information shows the most tremulant data.

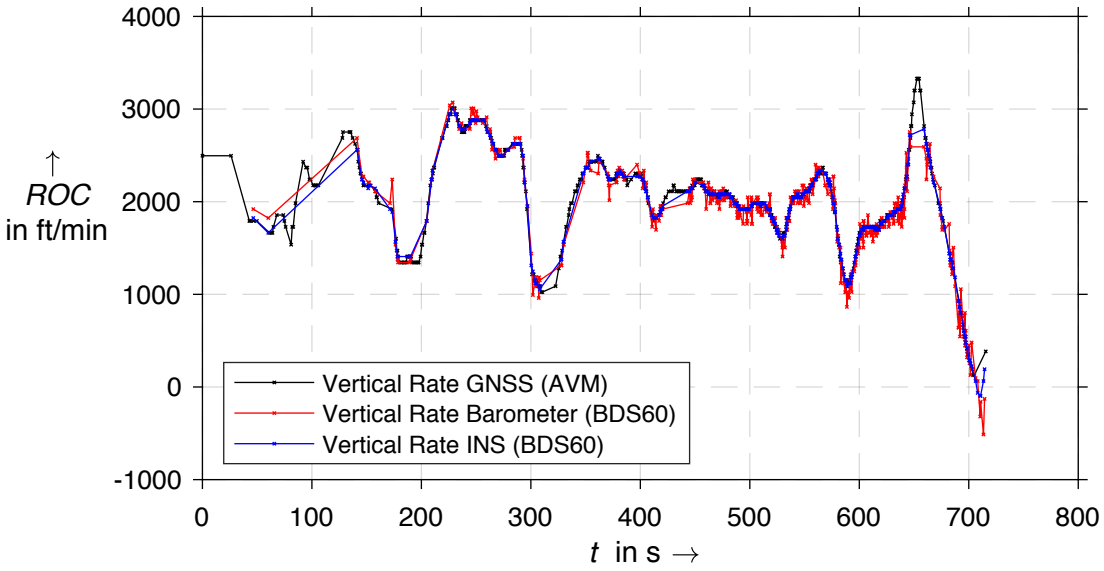

Figure 5.4 Vertical Rate

t	Time after first contact
ROC	Vertical rate

Figure 5.5 shows the different velocities ground speed, true airspeed, indicated airspeed as well as the Mach number. Ground speed and true airspeed show a similar progression. It can be seen

that the indicated airspeed shows a gentle progression and is almost constant between 330 s and 700 s. This correlates with the climb phase of the aircraft as the air density decreases. (**Skybrary 2020e**)

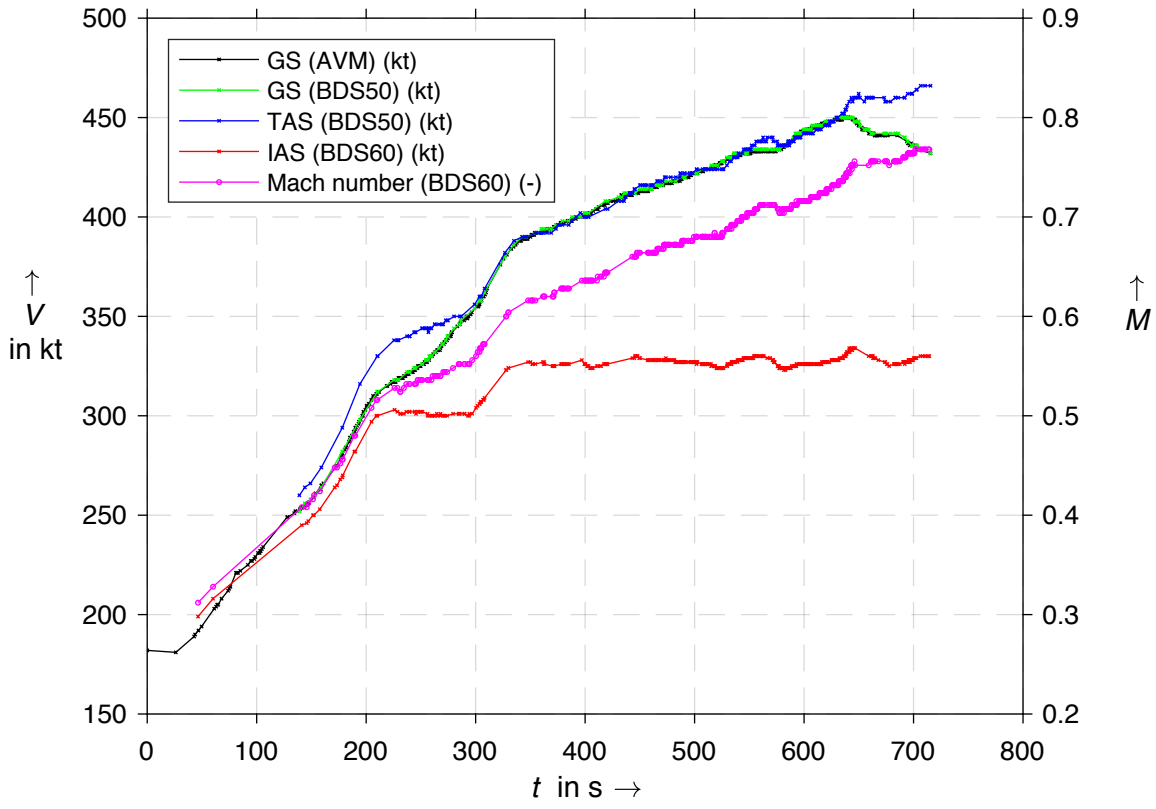

Figure 5.5 Speed information

t	Time since first contact
V	Velocity
M	Mach number

Figure 5.6 shows the magnetic heading, the true track angle, the selected heading as well as the track angle rate. One can see that the track angle rate corresponds to the aircraft turns. It is noticeable that in this case the selected heading is adjusted just after the aircraft has established a stable flight with the corresponding heading.

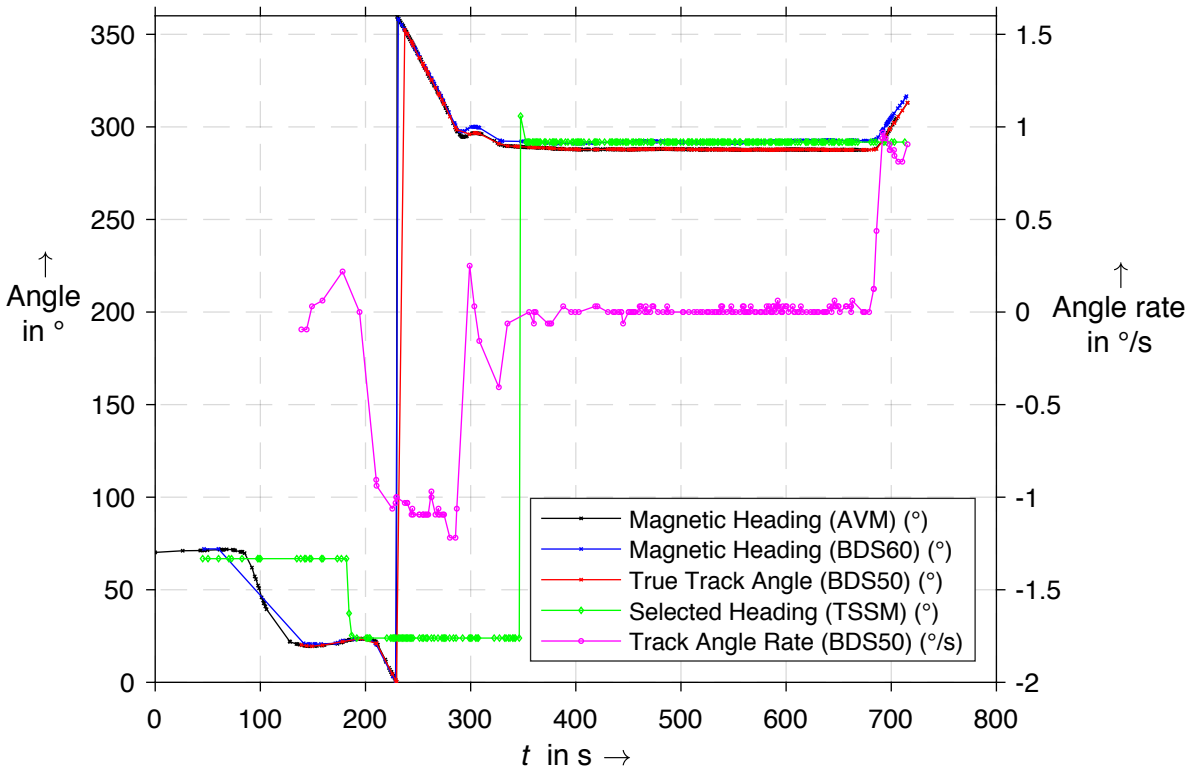

Figure 5.6 Heading information

t Time since first contact

In Figure 5.7 the roll angle data is depicted. The roll angle shows a similar progression as the track angle rate in Figure 5.6.

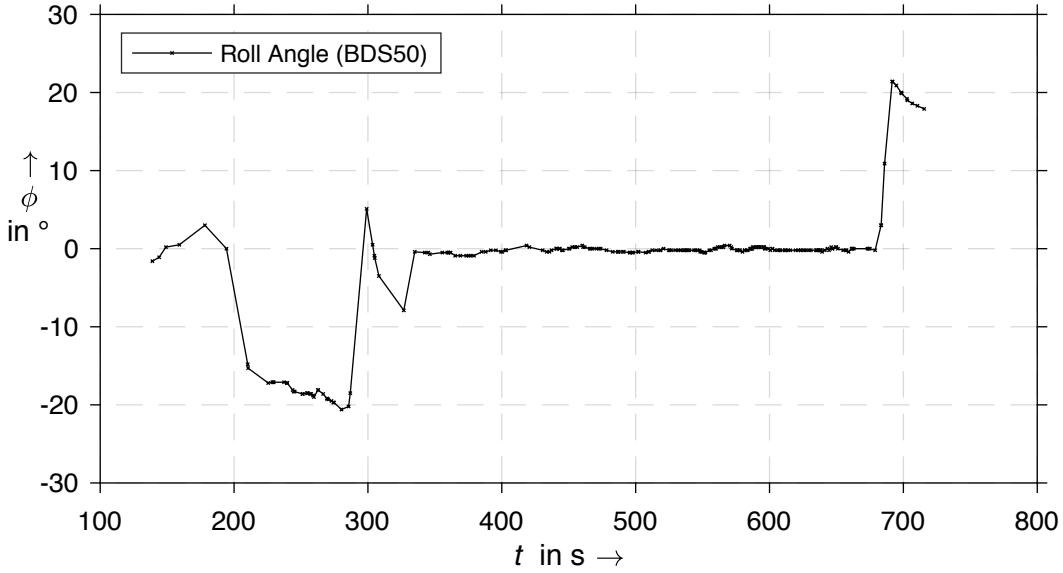

Figure 5.7 Roll angle

t Time since first contact
ϕ Roll angle

Figure 5.8 shows the airborne status of the example flight. The aircraft was airborne during the whole time the receiver received messages from this aircraft.

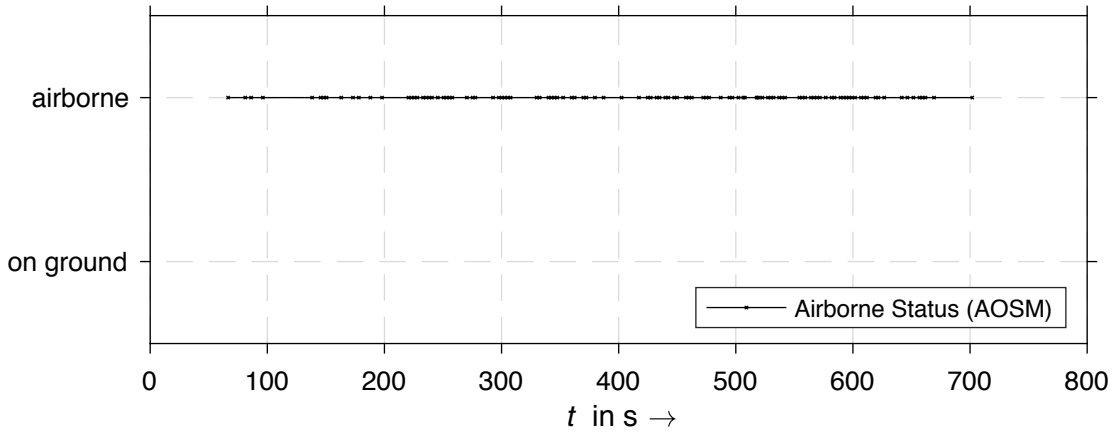

Figure 5.8 Airborne status

t Time since first contact

Figure 5.9 to Figure 5.12 depict several autopilot statuses. While Figure 5.9 shows that the autopilot itself has been engaged at approx. 175 s after the first contact with this aircraft. Figure 5.10 shows that VNAV mode was engaged throughout the considered flight section. Figure 5.11 and Figure 5.12 show that the altitude hold mode, as well as the approach mode, were disengaged. This is reasonable as the aircraft was in the climb phase throughout the considered flight section.

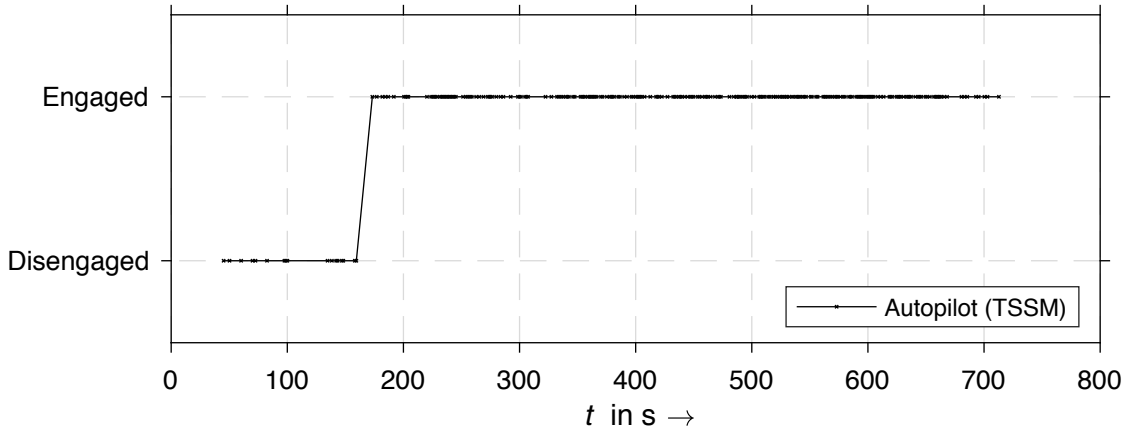

Figure 5.9 Autopilot status

t Time since first contact

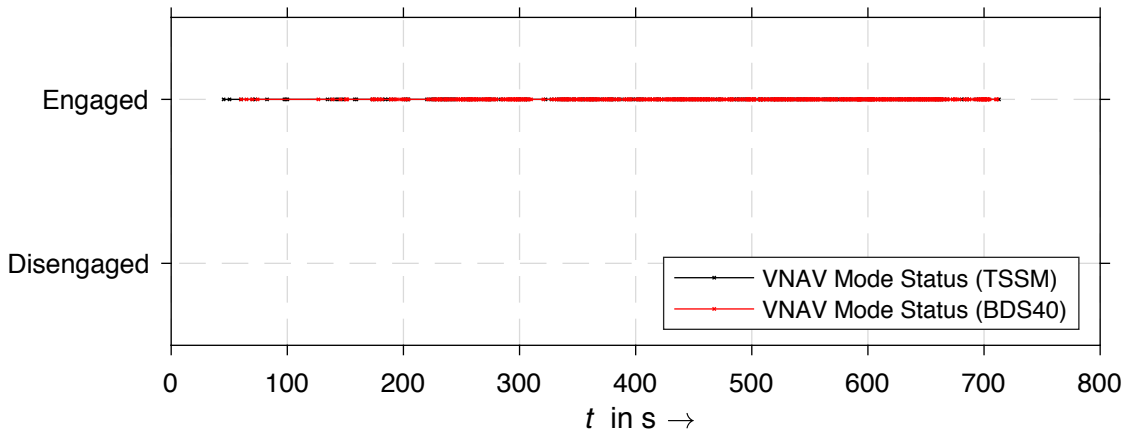

Figure 5.10 VNAV mode status

t Time since first contact

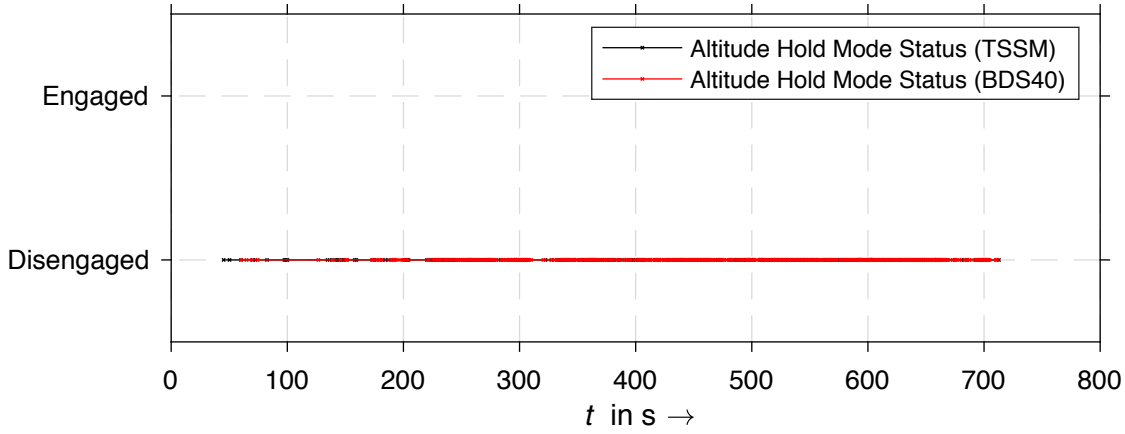

Figure 5.11 Altitude hold mode status

t Time since first contact

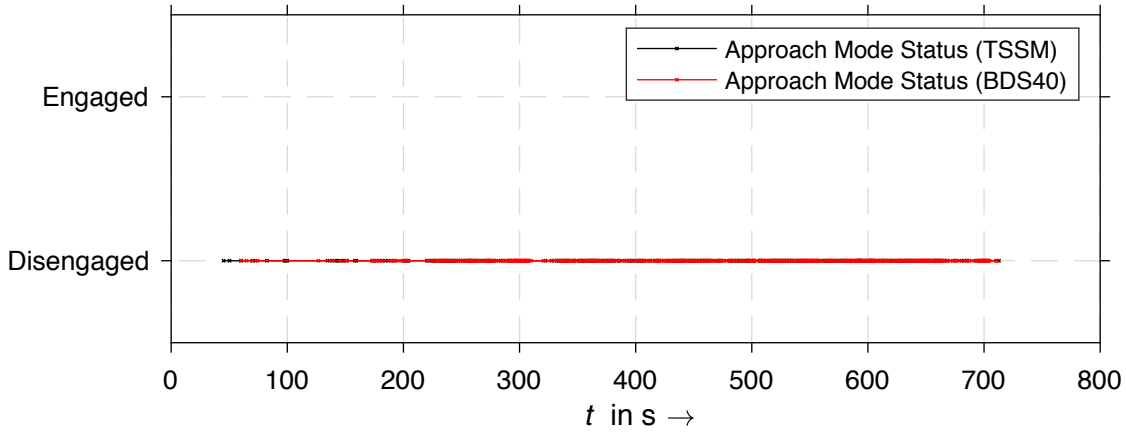

Figure 5.12 Approach mode status

t Time since first contact

5.5 Discussion of ADS-B and Mode S Data

The homebuilt set-up received approx. 4.87 ADS-B and other Mode S messages per second for a time frame of nearly 12 minutes. For the same time frame, the Flightradar24 CSV data contains 51 data sets for this specific flight. This represents an average of 0.07 data sets containing position, ground speed and direction information per second. This means that significantly more data is available using the homebuilt receiver, both in terms of broadcast rate and also the number of transmitted parameters.

Looking at the number of received ADS-B messages, it can be seen that the receiving rate (Table 5.8) is only less than half of the specified broadcast rate (Table 5.4). It is possible that this is due temporary lack of coverage or the inability for the receiver set-up to process all incoming messages. Nonetheless, the *airborne position message*, *airborne velocity message*, and *heading and speed report* were received almost every second, the *track and turn report* almost every three seconds. These messages contain those parameters that can change quickly.

The additional parameters, compared to the Flightradar24 data, are of high value for the aircraft performance analysis. Especially values like true airspeed and roll angle, as they describe the state of the aircraft. The indicated airspeed, part of the *heading and speed report* (BDS60) and the *air-referenced state vector* (BDS53) is the most important speed parameter when it comes to flight characteristics (**Skybrary 2020e**).

Further information regarding the aircraft and flight state, like the selected vertical intention, autopilot status, and barometric pressure setting, help to put the data into context. This offers an extensive picture of the aircraft and flight state. Meteorological information (BDS44 and BDS45) would also enable a view of the aircraft's current surrounding conditions. However, as seen in this example, not all aircraft are capable of transmitting this information.

In this example, approx. 9 % of Comm-B replies could not be processed automatically by the heuristic-probabilistic decoding method implemented in the pyModeS library. This only occurred with BDS registers 5,0 and 6,0. According to **Sun 2019**, this is due to a similar message structure.

Besides, several other Comm-B messages exist as described in **EASA CS-ACNS** and **ICAO 9871**. This untapped potential could be used if they were implemented in the decoding software. However, data most relevant for aircraft performance can already be decoded. Further, it is uncertain how often these messages are interrogated by ground stations.

6 Summary and Conclusion

Since ADS-B has become more and more widespread in recent years, following several mandates in different regions worldwide, new possibilities to obtain aircraft data during flight opened up.

In Chapter 3, it has been looked at several potential aircraft and flight analyses. It has been evaluated whether the data provided by Flightradar24 is suitable for these. Due to the limited number of parameters and the comparatively low data rate, it is difficult to use the data for analyses in which certain missing parameters, like true airspeed, are essential or provided parameters, like ground speed, change quickly. However, Flightradar24 has an extensive network of ADS-B receivers and therefore offers a high coverage of flights worldwide. That is why this data is best suitable for macroscopic analyses not depending on high data rates, but for which worldwide coverage is desirable and for which position, ground speed, altitude, and direction are sufficient.

Chapter 4 has given an example of this kind of analysis by taking a closer look at initial cruise altitudes and step climbs of different aircraft types. As only altitude and time information is needed and the aircraft's altitude does not change quickly during the cruise phase, Flighradar24 provides sufficient data. It has been concluded that, in most cases, the same tendencies have been found for all aircraft types. The initial cruise altitude decreases, and the number of steps increases with the increase in flight distance. To better understand the differences between the aircraft types, larger sample sizes are needed. Besides, potential difficulties, like the lack of coverage during the cruise phase, have been addressed.

Chapter 5 has given an overview of the parameters contained in ADS-B and Comm-B messages. Using an open-source library, a script to decode this data has been developed. The data of an example flight has been received via a homebuilt set-up. It has been shown that this method provides significantly more parameters at a higher data rate. This allows a more detailed analysis, and a more complete picture of the aircraft and flight state is created by additional autopilot, system and weather information. Nevertheless, one has to keep in mind that receiving extended Mode S data depends on the capability of the transponder and the interrogation by ground stations. Further, the coverage of a single receiver is limited. With better equipment, especially better antenna and antenna position, an increase in range could be achieved. Still, it is unlikely that covering a complete flight from origin to destination airport with only one receiver is possible.

These observations lead to the conclusion that one mainly has to decide between the number of parameters, data rate and coverage. Flightradar24 offers wide coverage but limited parameters. A homebuilt receiver shows a higher potential in terms of the amount of data but at a limited

coverage. These limitations have to be kept in mind when choosing a data source for flight, and aircraft performance analysis.

References

AVHERALD.COM, 2019. *Incident: Malta A320 at London on Sep 21st 2019, rejected takeoff due to bird strike*.
Available from: https://avherald.com/h?article=4cd21909,
Archived at: https://perma.cc/KH7H-WBJ9.

EUROPEAN AVIATION SAFETY AGENCY (EASA), 2018a. *Seasonal Technical Communication*. Cologne: European Aviation Safety Agency.
Available from: https://bit.ly/2Ub2oGs,
Archived at: https://perma.cc/BG6K-TBCU.

EUROPEAN AVIATION SAFETY AGENCY (EASA), 2018b. *ADS-B and other means of surveillance implementation status*.
Available from: https://bit.ly/39Zvuz5,
Archived at: https://perma.cc/K7H3-5QLS.

EUROPEAN AVIATION SAFETY AGENCY (EASA), 2019. EASA CS-ACNS: *Certification Specifications and Acceptable Means of Compliance for Airborne Communications, Navigation and Surveillance.* Issue 2.
Available from: https://bit.ly/2wP9yrS,
Archived at: https://perma.cc/K5A7-7ZNY.

FLIGHTRADAR24.COM, 2019a. *The Evolution of Flightradar24 Coverage*.
Available from: https://bit.ly/2Q5N1h6
Archived at: https://perma.cc/ZEU2-MWA2.

FLIGHTRADAR24.COM, 2019b. *British Airways flight BA280*.
Available from: https://www.flightradar24.com/data/flights/BA280#22b20f08,
Archived at: https://perma.cc/ENX7-5PD6.

FLIGHTRADAR24.COM, 2020a. *How flight tracking works*.
Available from: https://www.flightradar24.com/how-it-works,
Archived at: https://perma.cc/KQN7-N5V8.

FLIGHTRADAR24.COM, 2020b. *Flightradar24's 2019 by the numbers*.
Available from: https://bit.ly/2TLx5Ti,
Archived at: https://perma.cc/QVT8-7CKQ.

FLIGHTRADAR24.COM, 2020c. *Subscription plans*.
Available from: https://www.flightradar24.com/premium/,
Archived at: https://perma.cc/38RM-ABU7.

INTERNATIONAL CIVIL AVIATION ORGANIZATION (ICAO), 2005. *Annex 2 to the Convention on International Civil Aviation – Rules of the Air*. Tenth edition. Montréal: International Civil Aviation Organization.
Available from: https://bit.ly/2xS5cRf,
Archived at: https://perma.cc/L6VB-ZGD6.

INTERNATIONAL CIVIL AVIATION ORGANIZATION (ICAO), 2012. ICAO 9871: *Technical Provisions for Mode S Services and Extended Squitter*. 2nd edition. Montréal: International Civil Aviation Organization. ISBN 978-9-29-249042-3

INTERNATIONAL VIRTUAL AVIATION ORGANIZATION (IVAO), 2020. *Frankfurt Main Airport Details*.
Available from: https://bit.ly/3dcWfCd,
Archived at: https://perma.cc/X5V7-JD6N.

KLEDER, Michael, 2019. *Geodetic distance on WGS84 earth ellipsoid*. MATLAB Central File Exchange.
Available from: https://bit.ly/2TZO6rZ,
Archived at: https://perma.cc/3DTQ-W8PH.

MATLAB, 2020a. *azimuth*.
Available from: https://www.mathworks.com/help/map/ref/azimuth.html,
Archived at: https://perma.cc/59VA-8RMK.

MATLAB, 2020b. *Box plot*.
Available from: https://www.mathworks.com/help/stats/boxplot.html,
Archived at: https://perma.cc/R7A9-WC8P.

OPENFLIGHTS.ORG, 2020. *Airport and Airline Data*.
Available from: https://openflights.org/data.html,
Archived at: https://perma.cc/59PD-X5JQ.

SKYBRARY.COM, 2020a. *Automatic Dependent Surveillance-Broadcast (ADS-B)*.
Available from: https://bit.ly/3cQR8r6,
Archived at: https://perma.cc/JT5K-QUEU.

SKYBRARY.COM, 2020b. *London Heathrow Airport*.
Available from: https://www.skybrary.aero/index.php/EGLL,
Archived at: https://perma.cc/98C2-M6YV.

SKYBRARY.COM, 2020c. *Altitude, Flight Level and Height*.
Available from: https://bit.ly/38TrnTZ,
Archived at: https://perma.cc/7GXZ-EMQP.

SKYBRARY.COM, 2020d. *Mode S*.
Available from: https://www.skybrary.aero/index.php/Mode_S,
Archived at: https://perma.cc/3QQK-WBZB.

SKYBRARY.COM, 2020e. *Indicated Airspeed (IAS)*.
Available from: https://bit.ly/2Qw05g8,
Archived at: https://perma.cc/SYJ2-PUP4.

SUN, Jinzu; VÛ, Huy; ELLERBROEK, Joost; et al., 2019. pyModeS: Decoding Mode S Surveillance Data for Open Air Transportation Research. In: *IEEE Transactions on Intelligent Transportation Systems*.
Available from: http://doi.org/10.1109/TITS.2019.2914770 (Open Access)

THISDELL, Dan and SEYMOUR, Chris, 2019. World Airliner Census 2019. In: *Flight International.* 2019-07-30, vol. 196, no. 5697, pp. 28-47.
Archived at: https://perma.cc/K53V-QAQS.

YOUNG, Trevor, 2001. *Lecture Notes Flight Mechanics.* Department of Mechanical and Aeronautical Engineering, University of Limerick.